TURUN YLIOPISTO
Matemaattis-luonnontieteellinen tiedekunta

MAGNETOSTATIC MODES IN SPIN-POLARIZED ATOMIC HYDROGEN

LAURI LEHTONEN

THEORETICAL PHYSICS
MASTER'S THESIS
CREDITS:30

SUPERVISORS:
Kalle-Antti Suominen
Sergei Vasiliev

29.3.2023
Turku, Finland

欲速，则不达；见小利，则大事不成。

Crave haste, and never finish; only see small gains, and never attain large ones.

— The Analects

ABSTRACT

TURUN YLIOPISTO
Matemaattis-luonnontieteellinen tiedekunta

MASTER'S THESIS
SUBJECT: Theoretical Physics
AUTHOR: Lauri Lehtonen
TITLE: Magnetostatic Modes in Spin-Polarized Atomic Hydrogen
SUPERVISORS: Kalle-Antti Suominen, Sergei Vasiliev
NUMBER OF PAGES: 74
DATE: 29.3.2023

Magnetostatic modes are considered as a potential explanation for certain features of the electron spin resonance spectra observed in a gas of spin-polarized atomic hydrogen. The resonance spectra were measured in the Turku atomic hydrogen group. Magnetostatic modes are wave-like perturbative solutions of a disturbed oscillating magnetized medium described by the Walker equation [37]. In this work, analytic solutions for the Walker equation are found in the experimentally relevant finite cylindrical geometry by imposing extra boundary conditions on the infinite cylinder [21]. Unfortunately the model turns out to be unable to account for the observed modulations of the spectra, and the modulations it could produce are likely too narrow to be seen with the experimental apparatus.

KEYWORDS: spin waves, atomic hydrogen, magnetostatic waves, electron spin resonance, Walker's equation, cold atoms.

TIIVISTELMÄ

TURUN
YLIOPISTO
Matemaattis-luonnontieteellinen
tiedekunta

PRO GRADU -TUTKIELMA
PÄÄAINE: Teoreettinen fysiikka
TEKIJÄ: Lauri Lehtonen
OTSIKKO: Magnetostatic Modes in Spin-Polarized Atomic Hydrogen
OHJAAJAT: Kalle-Antti Suominen, Sergei Vasiliev
SIVUMÄÄRÄ: 74
PÄIVÄMÄÄRÄ: 29.3.2023

Tutkielmassa tutkitaan mahdollisuutta selittää eräitä spin-polaroidussa atomisessa vetykaasussa havaitun elektroni-spin-resonanssispektrin piirteitä magnetostaattisten värähtelymoodien avulla. Spektri on mitattu Turun atomisen vedyn ryhmässä; tutkielman kirjoittaja ei osallistunut mittaustyöhön. Magnetostaattiset värähtelymoodit ovat oskilloivan magneettisen aineen aaltomaisia häiriöratkaisuja, joita kuvataan Walkerin yhtälöllä [37]. Tässä tutkielmassa Walkerin yhtälö ratkaistaan analyyttisesti kokeen äärellisessä sylinterissä lisäämällä reunaehtoja äärettömän sylinterin ratkaisuihin [21]. Valitettavasti malli ei kykene selittämään spektrin havaittuja erikoispiirteitä, ja sen mahdolliset vaikutukset siihen lienevät terävyytensä takia koejärjestelmän ulottumattomissa.

AVAINSANAT: spin-aallot, atominen vety, magnetostaattiset aallot, elektronispinresonanssi, Walkerin yhtälö, kylmät atomit.

PUBLICATIONS

Some ideas and figures have appeared previously in the following publications:

[1] L. Lehtonen, O. Vainio, J. Ahokas, J. Järvinen, S. Sheludyakov, K.-A. Suominen, and S. Vasiliev. "Searching for magnetostatic modes in spin-polarized atomic hydrogen." In: *Physica Scripta* 95.4 (Feb. 2020), p. 045405. DOI: 10.1088/1402-4896/ab6eb4.

CONTENTS

LIST OF FIGURES

Part I

INTRODUCTION

1 THE ORIGINS OF SPIN WAVES

1.1 MAGNETISM

In a discussion of spin waves one can hardly avoid mentioning magnetism, for magnetization is the macroscopic manifestation of the large-scale alignment of spins (or magnetic moments), the environment wherein spin waves propagate. Indeed, it is perhaps more intuitive to speak of long-wavelength spin waves (such as magnetostatics waves) as the macroscopic variation of magnetization rather than that of propagation of spin perturbations.

Magnetic materials have been known to man for thousands of years: possibly the first lodestone compass (most likely used for geomancy) belonged to the Olmecs already around 1000BCE[8]; the first mention from the Chinese dates back to the 3rd century BCE[8]. In Europe, The Greek philosopher Thales (c. 600BC) knew of lodestone's power to attract iron[8].

Nowadays quantum mechanics is regarded as a central component of magnetism. This became especially clear in the early 20th century, when the Bohr–van Leeuwen theorem questioned the origins of magnetism: it showed that classical statistical mechanics and electrodynamics were incompatible with magnetism, as they implied that the thermal average of magnetization should always be zero, so no magnets could exist. Quantization of the electron motion and their magnetic moments was needed to overcome the theorem. [31]

Magnetization of a system characterizes its response to an external applied field. It is defined as the magnetic dipole moment density of the system[34], where magnetic dipoles are taken to be the fundamental 'atoms' of magnetization, the elementary bar magnets. In old quantum physics, these dipoles were thought to arise (semiclassically) from electrons orbiting the atom in quantized Bohrian orbits, the movement of electrons being an electric current that, through Faraday's law, produces a magnetic field. Today it is acknowledged that the movement of the electron does contribute to the magnetic moment of an atom as shown by the Einstein-de Haas effect[14, 15, 30], but it is usually neither its only nor its primary source.

In new quantum mechanics, an atom has a dipole moment due to electron motion and the spins of its constituent particles. Mathematically, the spin observable arises from a quantum mechanical treatment of Galilei- or Lorentz-invariant systems, but not from a classical treatment; hence it is said to be a purely quantum mechanical observable. While both spin and angular momentum are properties of

a rotationally invariant systems such as Galilei- or Lorentz-invariant systems, the spin has no classical analogue, though it has a classical manifestation as the magnetic moment of a particle. This is because the spin interacts with the magnetic field[1] in a way that confers a particle an intrinsic magnetic moment of magnitude $\vec{\mu}_S = \gamma\vec{S}$, where the constant of proportionality γ is variously called the gyromagnetic ratio, magnetomechanical ratio, or magnetogyric ratio. In an atom, both the electrons and the nucleus have a spin, though owing to the mass of the nucleus its magnetic moment is typically around 1000 times smaller than that of the electron, so its contribution to the total magnetization of the material is usually negligible. Dynamically the nuclear spin may still play an important role as it does in NMR spectroscopy.

Magnetic materials can be loosely grouped by the order exhibited by their magnetic moments[34, p. 1-3].

- Materials without permanent magnetic moments are *diamagnets*: when placed in an external field, they magnetize so as to minimize the applied field.
- *Paramagnets* have magnetic moments without any order without applied field: when a field is applied, the material organizes to produce a magnetic moment in the direction of the field.
- In *ferromagnets*, permanent magnetic moments are aligned within larger domains, and the domains align upon application of magnetic field. The spontaneous alignment of spins within the domain is caused by the exchange interaction arising from the overlap of neighbouring wave functions.
- *Ferrimagnets* contain two or more sublattices having unequal magnetic moments, and the total magnetic moment is determined by their sum. Typically, the field produced by such substances in applied field is weaker than that of ferromagnets.
- In *antiferromagnets*, the magnetic moments of the sublattices cancel exactly. Theoretically, if the applied field is aligned with the magnetic moments, such substances produce no magnetic field, although in practice there is a small contribution owing to thermal fluctuations. However, if the field is applied perpendicular to the moments, all the lattices tend to align with the field, thus producing magnetization.

The subject of this work is spin-polarized atomic hydrogen, which is a gas and as such has no magnetic order, so it is a paramagnet. Its magnetic moment is essentially due to the electron spin, hence the spin waves could be called electron spin waves. The nuclear spin plays

1 Or more accurately, the spin interacts with the underlying scalar and vector potentials as shown by the Aharonov-Bohm effect[2]

an important role in the scattering and recombination dynamics of the gas, but for the purposes of this work it is negligible.

1.2 SPIN WAVES

The idea of spin waves seems to trace back to F. Bloch's[5] work in the early 1930s in the context of characterization of ferromagnetism. In 1907, to explain the hysteresis and saturation magnetization of ferromagnets, Weiss[38] had proposed that ferromagnets are composed of domains within which the elementary magnets are aligned by the molecular magnetic field produced by the other magnets in the domain. An elementary magnet in the domain would not experience just the external field $\vec{H}$, but also the molecular field $q\vec{M}$, where q is a constant of proportionality. The molecular field can account for the temperature dependence of magnetization as well as the persistence of magnetization with $\vec{H} = 0$ in face of thermal fluctuations, while the unaligned domains could account for magnetizations less than that of the saturation magnetization [1].

The origin of the molecular field remained a mystery. How could the elementary magnets align to produce the field observed? The only candidate was the classical dipolar interaction, which turned out to be too weak: it predicted a value of $q \leq 4\pi$, while experiments required values in excess of 10^5. In addition, the theory predicts that q depends on how the sample is cut and the orientation of the field relative to the crystallographic axes, while experiments seemed to be relatively insensitive to these [36]. The solution was found in the spin–spin interactions embodied in the Heisenberg Hamiltonian $H = \sum_{i,j} J_{ij} S_i \cdot S_j$. The exchange interaction, from which the Hamiltonian derives, is sufficiently strong to align the spins within the domains. However the Heisenberg system is not solvable exactly, so the thermodynamic behaviour of various quantities, such as saturation magnetization, cannot be predicted accurately. It was in examining the Heisenberg system that Bloch, motivated by Slater's observations, came to consider spin configurations with one flipped spin. He found solutions propagating in the lattice, and using their dispersion relation Bloch was able to derive his eponymous $T^{\frac{3}{2}}$ law for magnetization at low temperatures.

As an example, consider a simple chain of N equidistant spin$-\frac{1}{2}$ particles whose dynamics are governed by the Heisenberg Hamiltonian([34, p. 46]):

$$\mathbf{H} = -\frac{J}{\hbar^2} \sum_{n=1}^{N} \mathbf{S}_n \cdot \mathbf{S}_{n+1}.$$

With the usual definition of the ladder operators

$$\begin{aligned}\mathbf{S}^+ =&\mathbf{S}^x + i\mathbf{S}^y = \hbar\,|\uparrow\rangle\langle\downarrow|\\ \mathbf{S}^- =&\mathbf{S}^x - i\mathbf{S}^y = \hbar\,|\downarrow\rangle\langle\uparrow|\\ \mathbf{S}^z =&\frac{\hbar}{2}\,|\uparrow\rangle\langle\uparrow| - \frac{\hbar}{2}\,|\downarrow\rangle\langle\downarrow|\end{aligned}$$

and the relation

$$\begin{aligned}&\mathbf{S}_i^+\mathbf{S}_j^- + \mathbf{S}_i^-\mathbf{S}_j^+\\ =&\mathbf{S}_i^x\mathbf{S}_j^x + \mathbf{S}_i^y\mathbf{S}_j^y + \cancel{i\left(\mathbf{S}_j^x\mathbf{S}_i^y - \mathbf{S}_i^x\mathbf{S}_j^y\right)}\\ +&\mathbf{S}_i^x\mathbf{S}_j^x + \mathbf{S}_i^y\mathbf{S}_j^y - \cancel{i\left(\mathbf{S}_j^x\mathbf{S}_i^y - \mathbf{S}_i^x\mathbf{S}_j^y\right)}\\ =&2\left(\mathbf{S}_i^x\mathbf{S}_j^x + \mathbf{S}_i^y\mathbf{S}_j^y\right),\end{aligned}$$

the Hamiltonian can be rewritten as a sum of $\mathbf{S}_n^z$ and the spin flip operators $\mathbf{S}_n^+\mathbf{S}_{n+1}^-$:

$$\begin{aligned}\mathbf{H} =& -\frac{J}{\hbar^2}\sum_{n=1}^{N}\left(\mathbf{S}_n^x\mathbf{S}_{n+1}^x + \mathbf{S}_n^y\mathbf{S}_{n+1}^y + \mathbf{S}_n^z\mathbf{S}_{n+1}^z\right)\\ =& -\frac{J}{\hbar^2}\sum_{n=1}^{N}\left(\mathbf{S}_n^x\mathbf{S}_{n+1}^x + \mathbf{S}_n^y\mathbf{S}_{n+1}^y + \mathbf{S}_n^z\mathbf{S}_{n+1}^z\right)\\ =& -\frac{J}{2\hbar^2}\sum_{n=1}^{N}\left(\mathbf{S}_n^+\mathbf{S}_{n+1}^- + \mathbf{S}_n^-\mathbf{S}_{n+1}^+ + 2\mathbf{S}_n^z\mathbf{S}_{n+1}^z\right).\end{aligned}$$

The system is in the ground state when all spins are pointing down ($J > 0$), so the ground state energy is given by

$$\begin{aligned}\mathbf{H}\,|\downarrow\ldots\downarrow\rangle =& -\frac{J}{2\hbar^2}\sum_{n=1}^{N}\left(0 + 0 + 2\frac{\hbar^2}{4}\right)|\downarrow\ldots\downarrow\rangle\\ =& -\frac{NJ}{4}\,|\downarrow\ldots\downarrow\rangle.\end{aligned}$$

For clarity, it is useful to shift the ground state energy of the Hamiltonian to 0:

$$\begin{aligned}\mathbf{H}' =&\mathbf{H} + \frac{NJ}{4}\mathbf{I}\\ =&\frac{NJ}{4}\mathbf{I} - \frac{J}{2\hbar^2}\sum_{n=1}^{N}\left(\mathbf{S}_n^+\mathbf{S}_{n+1}^- + \mathbf{S}_n^-\mathbf{S}_{n+1}^+\right) - \frac{J}{\hbar^2}\sum_{n=1}^{N}\mathbf{S}_n^z\mathbf{S}_{n+1}^z\\ \mathbf{H}'\,|E_0\rangle =&\mathbf{H}'\,|\downarrow\ldots\downarrow\rangle = \mathbf{0}.\end{aligned}$$

For spin waves, consider states with one flipped spin, that is $S_i^+\,|\downarrow\ldots\downarrow\rangle$. As it turns out, these are not eigenstates of $\mathbf{H}'$. To

find the energy eigenstates with one flipped spin, one can use the coordinate Bethe Ansatz:

$$|E_1\rangle = |p\rangle = \frac{1}{\hbar\sqrt{N}} \sum_{k=1}^{N} e^{ipx_k} S_k^+ |\downarrow \dots \downarrow\rangle = \frac{1}{\sqrt{N}} \sum_{k=1}^{N} e^{ipka} |\downarrow \dots \uparrow_k \dots \downarrow\rangle .$$

Essentially, one supposes that the eigenstates are given by a Fourier sum of the states with one flipped spin with $x_k = ka$ the position of the spin, and p a number which one might guess to be a momentum. A short calculation shows that these are indeed eigenstates of the Heisenberg spin chain Hamiltonian:

$$\begin{aligned}
\mathbf{H}' |p\rangle =& \frac{NJ}{4} |p\rangle - \frac{J}{2\hbar^2} \sum_{n=1}^{N} \left(\mathbf{S}_n^+ \mathbf{S}_{n+1}^- + \mathbf{S}_n^- \mathbf{S}_{n+1}^+ \right) \frac{1}{\sqrt{N}} \sum_{k=1}^{N} e^{ipka} |\downarrow \dots \uparrow_k \dots \downarrow\rangle \\
& - \frac{J}{\hbar^2} \left(\sum_{n=1}^{N} \mathbf{S}_n^z \mathbf{S}_{n+1}^z \right) \frac{1}{\sqrt{N}} \sum_{k=1}^{N} e^{ipka} |\downarrow \dots \uparrow_k \dots \downarrow\rangle \\
=& \frac{NJ}{4} |p\rangle - \frac{J}{2\hbar^2} \frac{1}{\sqrt{N}} \sum_{n=1}^{N} \left(\delta_k^{n+1} \mathbf{S}_n^+ \mathbf{S}_{n+1}^- + \delta_k^n \mathbf{S}_n^- \mathbf{S}_{n+1}^+ \right) e^{ipka} |\downarrow \dots \uparrow_k \dots \downarrow\rangle \\
& - \frac{J}{\hbar^2} \left(\sum_{n \neq k, n+1 \neq k} \frac{\hbar^2}{4} \right) \frac{1}{\sqrt{N}} \sum_{k=1}^{N} e^{ipka} |\downarrow \dots \uparrow_k \dots \downarrow\rangle \\
& - \frac{J}{\hbar^2} \left(-\frac{\hbar^2}{4} \right) \frac{1}{\sqrt{N}} \sum_{n=1}^{N} \left(e^{ipna} |\downarrow \dots \uparrow_n \dots \downarrow\rangle + e^{ip(n+1)a} |\downarrow \dots \uparrow_{n+1} \dots \downarrow\rangle \right) \\
=& \frac{NJ}{4} |p\rangle - \frac{J}{2} \frac{1}{\sqrt{N}} \sum_{n=1}^{N} \left(e^{ip(n+1)a} |\downarrow \dots \uparrow_n \dots \downarrow\rangle + e^{ipna} |\downarrow \dots \uparrow_{n+1} \dots \downarrow\rangle \right) \\
& - \frac{(N-2)\,J}{4} |p\rangle + \frac{J}{4} \frac{1}{\sqrt{N}} \sum_{n=1}^{N} \left(e^{ipna} |\downarrow \dots \uparrow_n \dots \downarrow\rangle + e^{ip(n+1)a} |\downarrow \dots \uparrow_{n+1} \dots \downarrow\rangle \right) \\
=& \frac{J}{2} |p\rangle - \frac{J}{2} \left(e^{ipa} + e^{-ipa} \right) |p\rangle + \frac{J}{2} |p\rangle \\
=& J \left[1 - \cos(pa) \right] |p\rangle \\
=& 2J \sin^2 \frac{pa}{2} |p\rangle \\
E_1(p) =& 2J \sin^2 \frac{pa}{2} \approx J \frac{p^2 a^2}{2}.
\end{aligned} \tag{1.1}$$

It is instructive to have a look at the solution of the time-dependent Schrödinger equation for these states, which are easily solved given the time-independent solutions:

$$\begin{aligned}
\Psi(t,p) &= \psi(t)\,|p\rangle \\
i\hbar\frac{\mathrm{d}\Psi(t,p)}{\mathrm{d}t} &= \mathbf{H}'\Psi(t,p) \\
&= E_1(p)\,\psi(t)\,|p\rangle \\
\psi(t) &= e^{-\frac{iE_1(p)t}{\hbar}} \\
\Psi(t,p) &= \frac{1}{\sqrt{N}}\sum_{k=1}^{N} e^{i\left(px_k-\frac{E_1(p)t}{\hbar}\right)}\,|\downarrow\ldots\uparrow_k\ldots\downarrow\rangle \\
&= \frac{1}{\sqrt{N}}\sum_{k=1}^{N} e^{i(px_k-\omega t)}\,|\downarrow\ldots\uparrow_k\ldots\downarrow\rangle
\end{aligned}$$

with

$$\omega = \frac{E_1(p)}{\hbar}. \tag{1.2}$$

The time-dependent eigenstate is thus a superposition of wave-like states traveling to the right with wavenumber p and frequency ω. So although the Schrödinger equation is not a wave equation but a (probability) diffusion equation, one gets very wave-like solutions out of it, explaining the terminology for spin waves. Equations describing spin waves are often in fact diffusion equations.

With the dispersion relation (1.1) one can derive Bloch's $T^{\frac{3}{2}}$-law using classical thermodynamics, though the approach is not so simple as one might think at first glance. Some effort has been spent on showing that superpositions of spin waves really are a valid approximation at low temperature and that bound states do not qualitatively change the situation[23, p. 18]. In short:

- $E(n\text{-flipped spins}) \approx \sum_n E\,(1\text{-flipped spin})$, i.e. spin wave states with multiple flipped spins can be reasonably approximated as a sum spin waves with a single flipped spin
- the contribution of bound states is not relevant at low temperatures.

Spin waves thus follow Bose-Einstein statistics, and the particle counterpart (by wave-particle duality) is called magnon. The $T^{\frac{3}{2}}$-law is obtained by summing over all momentum states using the Bose-Einstein distribution[23, p. 21]:

$$n(T) = \int_0^\infty \frac{\mathrm{d}^3p}{e^{\frac{E_1(p)}{k_BT}}-1} \approx \int_0^\infty \frac{\mathrm{d}^3p}{e^{\frac{Jp_x^2a^2}{2k_BT}+\frac{Jp_y^2a^2}{2k_BT}+\frac{Jp_z^2a^2}{2k_BT}}-1}$$

$$k_i = \sqrt{\frac{Ja^2}{2k_BT}}\,p_i$$

$$\mathrm{d}p_i = \sqrt{\frac{2k_BT}{Ja^2}}\,\mathrm{d}k_i$$

$$\int_0^\infty \frac{\mathrm{d}^3 p}{e^{\frac{Jp_x^2a^2}{2k_BT}+\frac{Jp_y^2a^2}{2k_BT}+\frac{Jp_z^2a^2}{2k_BT}}-1} = \left(\frac{2k_BT}{Ja^2}\right)^{\frac{3}{2}} \int_0^\infty \frac{\mathrm{d}^3 k}{e^{k_x^2+k_y^2+k_z^2}-1}.$$

The rest of the integral is just a number that turns out to be $2\pi\Gamma\left(\frac{3}{2}\right)\zeta\left(\frac{3}{2}\right)$. At low temperatures above absolute zero, every excited spin wave reduces the saturation magnetization, so the total magnetization is given by

$$M_s(T) = M_0\left[1-\frac{2\pi}{N_0}\Gamma\left(\frac{3}{2}\right)\zeta\left(\frac{3}{2}\right)\left(\frac{2k_BT}{Ja^2}\right)^{\frac{3}{2}}\right].$$

Hence, the magnetization of the sample is decreased by spin waves by a factor proportional to $T^{\frac{3}{2}}$ in this approach.

1.3 SPIN PRECESSION

As mentioned previously, the spin of a system interacts with the external magnetic field. In particular in atoms the magnetic field creates energy level differences between different spin states: this is known as the Zeeman effect. In quantum mechanics, the Zeeman effect is described through adding a Zeeman term of form $-\vec{\mu}_M \cdot \vec{B}$ to the Hamiltonian. For a Galilei-invariant spin-$\frac{1}{2}$ system in classical space $\mathbb{R}^3 \times \mathbb{R}$ in a magnetic field (a model for an electron, say), the spin interaction part of the Schrödinger equation can be formulated approximately in the following form:

$$i\hbar\frac{\partial\Psi}{\partial t} = \frac{e\hbar}{2mc}B_z\sigma_z\Psi$$

with

e charge of the system

m mass of the system

c speed of light

$\hbar$ reduced Planck constant

B_z magnetic field (chosen to be in the direction of the positive z-axis)

σ_z the third Pauli matrix.

Using for example the eigendecomposition, the solution of the Schrödinger equation is found straightforwardly:

$$
\begin{aligned}
\Psi(t) =& e^{-i\frac{e}{2mc}B_z t}\begin{pmatrix} c_1 \\ 0 \end{pmatrix} + e^{i\frac{e}{2mc}B_z t}\begin{pmatrix} 0 \\ c_2 \end{pmatrix} \\
=& \begin{pmatrix} c_1 e^{-i\frac{e}{2mc}B_z t} \\ c_2 e^{i\frac{e}{2mc}B_z t} \end{pmatrix} \\
E(\sigma_x) =& \begin{pmatrix} c_1 e^{-i\frac{e}{2mc}B_z t} \\ c_2 e^{i\frac{e}{2mc}B_z t} \end{pmatrix}^* \cdot \sigma_x \cdot \begin{pmatrix} c_1 e^{-i\frac{e}{2mc}B_z t} \\ c_2 e^{i\frac{e}{2mc}B_z t} \end{pmatrix} \\
=& \begin{pmatrix} c_1^* e^{i\frac{e}{2mc}B_z t} \\ c_2^* e^{-i\frac{e}{2mc}B_z t} \end{pmatrix} \cdot \begin{pmatrix} c_2 e^{i\frac{e}{2mc}B_z t} \\ c_1 e^{-i\frac{e}{2mc}B_z t} \end{pmatrix} \\
=& c_1^* c_2 e^{i\frac{e}{mc}B_z t} + \left(c_1^* c_2 e^{i\frac{e}{mc}B_z t}\right)^* \\
=& 2\,\mathrm{Re}\{c_1^* c_2\}\cos\left(\frac{eB_z}{mc}t\right) + 2\,\mathrm{Im}\{c_1^* c_2\}\sin\left(\frac{eB_z}{mc}t\right)
\end{aligned}
$$

So, in particular, if $c_1, c_2 \in \mathbb{R}$,

$$E(\sigma_x) = 2c_1 c_2 \cos\left(\frac{eB_z}{mc}t\right).$$

If the spin is not pointing up or down the z-axis ($c_1 \neq 0 \neq c_2$), the expectation value of the x-component of the spin oscillates; a similar equation applies to the y-component, and their combination describes precession of the spin around the z-axis. The frequency of the precession is proportional to the magnetic field B_z and the gyromagnetic ratio $\gamma = \frac{e}{mc}$. The exact relation is known as Larmor formula and the frequency is called the Larmor frequency:

$$\omega = \gamma B_z.$$

In spin waves, the intuition is (semiclassically) that the spins precess this way but with a constant phase shift between neighboring spins (Figure 1.1 on page 11). In context of the spin chain, the tilt of the spins is due to the one flipped spin which is shared by all the spins in the chain; in fact, $\langle S_i \rangle = \frac{\hbar}{2}\left(1 - \frac{1}{N}\right)$ (see [23, p. 16–17] for a more detailed discussion).

In magnetized media, one must somehow make the transition from a single spin to a continuum approach. The usual approach for a classical precessing magnetization is what are often called Landau-Lifshitz equations:

Landau-Lifshitz equations also include a damping term, which is left out.

$$\frac{\mathrm{d}\vec{M}}{\mathrm{d}t} = -\gamma \vec{M} \times \vec{H}_{\text{eff}}. \tag{1.3}$$

The quantities in this equation are the gyromagnetic ratio, the magnetization, and the effective field $\vec{H}_{\text{eff}}$. A simple solution of this equation can be found by assuming that $\vec{H}_{\text{eff}} = (0, 0, H_0)$, so

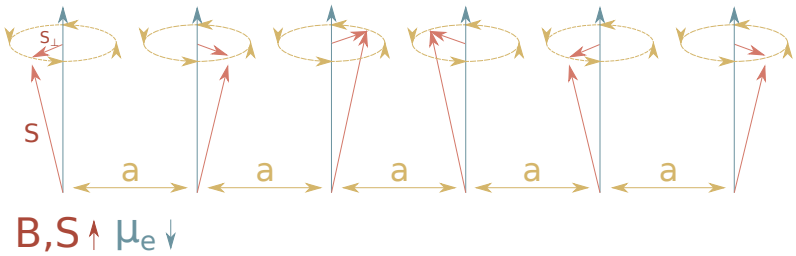

Figure 1.1: Semiclassical Picture of a Spin Wave

$$\left(\frac{\mathrm{d}M_x}{\mathrm{d}t}, \frac{\mathrm{d}M_y}{\mathrm{d}t}, \frac{\mathrm{d}M_z}{\mathrm{d}t}\right) = \gamma H_0 \left(-M_y, M_x, 0\right)$$
$$\frac{\mathrm{d}^2 M_x}{\mathrm{d}t^2} = -\gamma H_0 \frac{\mathrm{d}M_y}{\mathrm{d}t} = -\gamma^2 H_0^2 \frac{\mathrm{d}M_x}{\mathrm{d}t},$$

for which one oscillating solution is

$$\begin{aligned} M_x &= M_\perp \cos\left(|\gamma H_0|\, t\right) \\ M_y &= M_\perp \mathrm{sign}\left(\gamma H_0\right) \sin\left(|\gamma H_0|\, t\right) \\ M_z &= M_z. \end{aligned}$$

This is the background for ferromagnetic resonance and magnetostatic waves.

1.4 A BRIEF HISTORY OF FERROMAGNETIC RESONANCE AND MAGNETOSTATIC WAVES

The discovery of ferromagnetic resonance is attributed to Griffiths[16]. Like many of the specialists of his time, Griffiths had been involved in radar development during the second world war[35], and after the war used the expertise to perform experiments on ferromagnetic metals (Fe, Ni, Co) in microwave resonators. He used a metal sheet whereupon he applied a magnetic field in the plane of the sheet and an orthogonal microwave field (in the plane of the sheet), observing resonances at frequencies 2 to 6 times in excess of the calculated electron Larmor frequency. He suggested the Lorentz field may be the origin of the phenomenon, but Kittel soon dismissed this explanation and offered his own, based on an oscillating demagnetizing field[24]. This is known as the uniform mode or the Kittel mode. Kittel later extended his analysis to spheres and infinite cylinders and gave an account of the effect of crystalline anisotropy[25].

The Lorentz field, as far as I can tell, is just the demagnetizing field, i.e. the solution of $\nabla \cdot H_{demag} = -\nabla \cdot M$. *See section 2.2.*

Some years later observations of ferromagnetic resonance spectra with multiple peaks started appearing. White and Solt[39] offered early observations and an explanation in terms of higher-order non-uniform modes. Mercereau and Feynman[27] calculated some of those modes using physical intuition and guesswork under the assumption

of spatially-varying (non-uniform) magnetization. In 1957, Walker[37] changed and in retrospect defined the field by deriving his eponymous Walker equation for magnetostatic modes and solving it for a general ellipsoid. Afterwards solutions were found for the geometries where the demagnetizing field was simple, such as infinite sheets magnetized along the plane[11], infinite cylinder[21], and infinite disc[33] and rectangular films[32].

In this work we are interested in the cylindrical geometry, specifically a finite cylinder (where the demagnetizing field is not simple), so a review of the work on magnetostatics in cylinders is pertinent. Perhaps the first publication on the subject is by Kales[22], who determined that there are no TM, TE, or TEM resonator modes in a cylinder. He assumed an axial $e^{\gamma z}$ of the cylinder modes, and noted that there are modes when $\gamma = 0$. Damon[13] dealt with the demagnetizing field by using a constant demagnetizing factor in the axial direction and matching asymptotic solutions using the proper Maxwell boundary conditions. Bornmann[6] solved the cylinder modes assuming pinning boundary conditions. In addition, to deal with the demagnetizing field, a scheme to weight the demagnetizing factor using the spatial mode patterns was introduced. Bornmann also found that the azimuthal l and $-l$ modes were degenerate[2]. Corrucini[10] found plane wave solutions for a special case in a non-constant demagnetizing field.

On the experimental side, yttrium-iron-garnet (YIG) seems to have been the favorite substance to work with. Some interesting experiments were done by Damon[12], who measured spin wave echo delay as a function of magnetic field strength; the results agree well with the magnetostatic model. Corrucini[10] observed magnetostatic spin waves in cylindrical ^{3}He crystals. Rezende[29], again working with YIG, used magnetic microwave resonance in combination with Brillouin scattering to optically detect and image magnetostatic modes.

2 This is most likely due to the radial pinning boundary conditions.

Part II

SOLVING THE MODES

2

THE DEMAGNETIZING FIELD

2.1 MAGNETOSTATIC APPROXIMATION

In the experiments, atomic hydrogen is compressed in a cylindrical container with radius $r = 0.25\,\mathrm{mm}$. The length of the gas pillar varies depending on the phase of the compression cycle as the atomic hydrogen slowly recombines to hydrogen molecules, so the gas pillar may be considered to be a cylinder of variable length but fixed radius with its axis along the z-axis of the system.

A strong constant magnetic field $B_0\hat{\mathbf{e}}_z \sim 4.6\,\mathrm{T}$ is applied to the gas. In practice, due to some features of the setup the field is not entirely constant, however in some experiments these inhomogeneities were compensated for by applying magnetic field gradients. In addition to the applied field B_0, a weak, inhomogeneous, time-dependent rf field $\vec{h}_{\mathrm{ex}}(\vec{r},t)$ is applied to tilt the spins for electron spin resonance. The electromagnetic quantities of interest are thus the applied field $\vec{B}_0$, $\vec{h}_{\mathrm{ex}}(\vec{r},t)$, and of course the magnetization of the hydrogen gas $\vec{M}$, which is essentially equal to the saturation magnetization $M_0\hat{\mathbf{e}}_z$ due to the weakness of the exciting rf field.

To model the system, we seek solutions of Maxwell's equations in a cylinder (in Gaussian units):

$$\begin{aligned}
\nabla\cdot\vec{D} &= 4\pi\rho \\
\nabla\cdot\vec{B} &= 0 \\
\nabla\times\vec{E} &= -\frac{1}{c}\frac{\partial\vec{B}}{\partial t} \\
\nabla\times\vec{H} &= \frac{1}{c}\left(4\pi\vec{J}_f + \frac{\partial\vec{D}}{\partial t}\right).
\end{aligned}$$

The only external time-depence in the problem enters from the exciting rf-field (included in $\vec{B}$). Precessing mode solutions themselves are of course time-dependent as well, but these are treated as small quantities. The system does not have currents, so $\vec{J}_f = 0$. Owing to these reasons, the magnetostatic approximation is a valid model for the system. The magnetostatic approximation essentially consists of the following two assumptions:

$$\nabla\cdot\vec{B} = 0 \tag{2.1}$$

$$\nabla\times\vec{H} = 0 \tag{2.2}$$

The $\vec{E}$ and $\vec{D}$ fields are not of interest so they are left out. In Gaussian units, $\vec{B}$ and are $\vec{H}$ related by

$$\vec{B} = \vec{H} + 4\pi\vec{M} \tag{2.3}$$

where

$\vec{B}$ is given in Gauss $= 1 \times 10^{-4}\,\mathrm{T}$

$\vec{B}$ in Gauss and $\vec{H}$ in Oersted have equal magnitudes in Gaussian units, but not in SI units.

$\vec{H}$ is given in Oersted $= \frac{10^3}{4\pi}\mathrm{A\,m^{-1}}$

$\vec{M}$ is given in $\frac{\mathrm{emu}}{\mathrm{cm}^{-3}} = 1 \times 10^3\,\mathrm{A\,m^{-1}}$.

2.2 THE STATIC PROBLEM AND THE DEMAGNETIZING FIELD

Consider the situation in context of Equation 2.1 and Equation 2.2. Aside from the small quantity $\nabla \times \vec{h}_{\mathrm{ex}}$, Ampère's law is fulfilled because $\vec{H}_0$ is constant. Almost the same thing happens with Gauss's law, the only difference being due to the discontinuity of the magnetization:

$$\begin{aligned} 0 = \nabla \cdot \vec{B} =& \nabla \cdot (H_0 + 4\pi M_0)\,\hat{\mathbf{e}}_z + \nabla \cdot \vec{h}_{\mathrm{ex}} \\ \approx& 4\pi \frac{\partial M_0}{\partial z} = 0. \end{aligned}$$

As $\frac{\partial M_0}{\partial z}$ is not always zero (i.e. at the ends of the cylinder due to discontinuity of $M_0\,(z)$), another field is required to compensate for its contribution:

$$\vec{B} = \vec{H}_0 + 4\pi\vec{M}_0 + \vec{H}_{\mathrm{demag}}$$

where the new field, *the demagnetizing field*, or *the stray field*, fulfills the equation

$$\begin{aligned} \nabla \cdot \vec{H}_{\mathrm{demag}} =& -4\pi\nabla \cdot \vec{M} \\ =& -4\pi \frac{\partial M_0}{\partial z}. \end{aligned}$$

Further, by Ampère's law

$$0 = \nabla \times \left(H_0 \hat{\mathbf{e}}_z + \vec{H}_{\mathrm{demag}} \right) = \nabla \times \vec{H}_{\mathrm{demag}},$$

so $\vec{H}_{\mathrm{demag}} = \nabla\Psi$ for some function $\Psi\,(\vec{r})$. So we arrive at the Poisson equation

$$\nabla^2\Psi = -4\pi\nabla \cdot \vec{M}$$

whose solution is the following Green's function:

$$\Psi(\vec{r}) = -4\pi \int \frac{\nabla \cdot \vec{M}}{-4\pi \left|\vec{r} - \vec{r}'\right|} \mathrm{d}^3 r' \,. \tag{2.4}$$

As the situation mirrors that for the electric field generated by electric charges, $\nabla \cdot \vec{M}$ is sometimes referred to as the surface charge distribution in the case of uniformly magnetized systems, where the only contributions to $\nabla \cdot \vec{M}$ come from the discontinuites at the surfaces. Taking the analogy a step further, one can say that just as the electric field is the field generated by electric charges, the demagnetizing field is the magnetic field generated by the magnetization or the magnetic moments of the magnetized medium.

2.2.1 *Demagnetizating Factors*

In the simple case of a uniformly magnetized sphere of radius a, the Poisson equation reduces to Laplace equation with the usual Maxwell boundary conditions. The solutions can be given as series of Legendre polynomials P_l[17]:

$$\Psi = \begin{cases} \sum_{l=0}^{\infty} c_l r^l P_l(\cos\theta) & r < a \\ \sum_{l=0}^{\infty} d_l r^{-l-1} P_l(\cos\theta) & r > a \end{cases}$$

From the continuity of Ψ across the surface it follows that $d_l = c_l a^{2l+1}$, and from the continuity of the radial component of B it follows that $l = 1$ and $c_1 = \frac{-4\pi M}{3}$. The final solution is then

$$\Psi = \begin{cases} \frac{-4\pi M}{3} r\cos\theta & r < a \\ \frac{-4\pi a^3 M}{3} \frac{\cos\theta}{r^2} & r > a. \end{cases}$$

In Cartesian coordinates the solution inside the sphere is simply $\Psi = \frac{-4\pi M}{3} z$, and hence the field $\vec{H}_{\text{demag}} = -\frac{4\pi M}{3}\vec{e}_z$. The reason why it is called the demagnetizing field is now obvious: the field is directed against the magnetization and so acts to reduce it. The total field inside the sample is $H = H_0 - \frac{4\pi M}{3}$ in the z-direction. Owing to the simple relationship between the magnetization and the demagnetizing field one is tempted to define a demagnetizing factor, which for the case of the sphere is $\frac{1}{3}$. A similar result holds for ellipses: $H_k = (H_0)_k - 4\pi N_k M_k$ [28]. Generally, however, the demagnetizing field is non-uniform, so in practice one needs to consider a position-dependent demagnetization tensor (sometimes also called the *depolarization tensor*). In practice even this is as difficult as problems in magnetostatics tend to be. This is also the case for the cylinder, and so the non-uniformity

of the demagnetizing field both exacerbates the problem of finding the magnetostatic modes and raises the question of whether the modes even exist in a non-uniform background field.

One approach to this conundrum is to simply ignore it. One may hope that the effect of the non-uniform demagnetizing field compared to the external field is not significant, that the magnetostatic modes do not 'see' it. A slightly better approximation grants that there is a slight modulation of the external field owing to the demagnetizing field, but that the modulation can be seen as a constant shift proportional to the magnetization and some average of the demagnetizing field. Literature distinguishes between two such average demagnetizing factors for cylinders: the magnetometric N_m and the fluxmetric or ballistic N_f. N_m is defined as the ratio of average demagnetizing field to average magnetization in the volume V of the sample, while N_f is the same ratio but calculated only in the mid-plane S perpendicular to the cylinder's axis. The former is appropriate for small samples, while the latter is better suited for small search coils [9].

$$\int_V \vec{H}_d = -N_m \int_V M$$
$$\int_S \vec{H}_d = -N_f \int_S M$$

In the case of a small cylinder we are only interested in the axial magnetometric demagnetization factor N_z (also $\bar{N}_{zz}$ in literature, the average of the zz-component of the demagnetization tensor), as the magnetization is assumed to be uniform and the displacement owing to the magnetostatic modes negligible. The calculation of N_z can be done in at least three different ways: one can derive it from the self-inductance of a finite single-layer solenoid [7], use the theory of Joseph and Schlömann[19, 20], or one can use Fourier techniques [4]. As a result of some rather complicated calculations, for a cylinder of length L and radius r_c one obtains

$$N_z = 1 - \frac{8}{3\pi}\frac{r_c}{L}\left[-1 + \frac{1}{\varepsilon}\left(\frac{2\varepsilon^2 - 1}{\varepsilon^2}E(\varepsilon) + \frac{1-\varepsilon^2}{\varepsilon^2}K(\varepsilon)\right)\right] \tag{2.5}$$

$$\varepsilon^2 = \frac{1}{1 + \left(\frac{L}{2r_c}\right)^2} \tag{2.6}$$

Here $K(\varepsilon)$ and $E(\varepsilon)$ are the complete elliptical integrals of the first and second kind, respectively.

2.2.2 *Simple Magnetized Cylinder*

The equation for the demagnetizing field in the cylinder is given by

$$\nabla^2\Psi = -4\pi M_0 \nabla\left(\theta\left(z\right) - \theta\left(z-L\right)\right)$$

with θ the Heaviside function. The function in the parentheses is 1 within the cylinder, and 0 elsewhere. Evaluating the derivative gives

$$\nabla^2\Psi = -4\pi M_0 \left(\delta\left(z\right) - \delta\left(z-L\right)\right)$$

On the z-axis of the cylinder $r = 0$ the solution can be found using the Green function in Equation 2.4:

$$\begin{aligned}
\Psi =& 4\pi M \int \frac{\delta\left(z\right) - \delta\left(z-L\right)}{4\pi\sqrt{r^2 + \left(z-u\right)^2}} r\,\mathrm{d}r\,\mathrm{d}z\,\mathrm{d}\theta \\
=& 4\pi M \int \left[\frac{1}{2\sqrt{r^2+u^2}} - \frac{1}{2\sqrt{r^2+\left(u-L\right)^2}}\right] r\,\mathrm{d}r \\
=& -\frac{4\pi M}{2}\left(u - \sqrt{r_c^2+u^2} - \sqrt{L^2-2Lu+u^2} + \sqrt{L^2-2Lu+r_c^2+u^2}\right) \\
=& -\frac{4\pi M}{2}\left(u - \sqrt{r_c^2+u^2} - |L-u| + \sqrt{L^2-2Lu+r_c^2+u^2}\right) \\
=& -\frac{4\pi M}{2}\left(2u - L - \sqrt{r_c^2+u^2} + \sqrt{L^2-2Lu+r_c^2+u^2}\right)
\end{aligned}$$

The field is given by $\nabla\Psi$:

$$\begin{aligned}
h_z\left(0,\theta,u\right) = \frac{\mathrm{d}\Psi}{\mathrm{d}u} =& -\frac{4\pi M}{2}\left(2 - \frac{u}{\sqrt{r_c^2+u^2}} + \frac{-L+u}{\sqrt{L^2-2Lu+r_c^2+u^2}}\right) \\
\to& -4\pi M + \frac{4\pi M}{2}\frac{L}{\sqrt{r_c^2+L^2}} \quad \text{at the ends of the cylinder.}
\end{aligned} \tag{2.7}$$

So the total field at the ends of the cylinder would be

$$\begin{aligned}
B_z =& H_0 + 4\pi M + h_z \\
=& H_0 + \frac{4\pi M}{2}\frac{L}{\sqrt{r_c^2+L^2}} \\
\approx& H_0 + 2\pi M\left(1 - \frac{1}{2}\left[\frac{r_c}{L}\right]^2\right).
\end{aligned}$$

3

THE WALKER EQUATION AND ITS SOLUTIONS

3.1 THE WALKER EQUATION

The Walker equation is simply the Landau-Lifshitz equation (1.3) in the magnetostatic approximation, supplemented by the following ansatz:

$$\vec{H} = H\hat{\mathbf{e}}_z + \overbrace{(h_x, h_y, h_z)}^{\vec{h}} e^{i\omega t} \tag{3.1}$$

$$\vec{M} = M_0\hat{\mathbf{e}}_z + \underbrace{(m_x, m_y, 0)}_{\vec{m}} e^{i\omega t} \tag{3.2}$$

H here is the sum of the applied field and the demagnetizing field $H = H_0 + H_{\text{demag}}$. The demagnetizing field does have components also in other directions besides z, but in this work the demagnetizing field will either be ignored or incorporated via a demagnetizing factor as $H = H_0 - 4\pi M_0 N_z$.

Substituting $\vec{H} = H_0\hat{\mathbf{e}}_z + \vec{h}(\vec{r})$ into Equation 2.2, it follows that the equation also applies to $\vec{h}$: $\nabla \times \vec{h} = 0$. So there is a magnetic potential function such that $\vec{h} = \nabla\Psi$ and we can rewrite Equation 2.2 as

$$\nabla^2\Psi(\vec{r}) = 0. \tag{3.3}$$

$\vec{h}$ and $\vec{m}$ motivate the definition of $\vec{b} \equiv \vec{h} + 4\pi\vec{m}$, which also oscillates. Faraday's law would then give an approximation for the electric field:

$$\nabla \times \vec{e} = -i\omega\vec{b}. \tag{3.4}$$

To arrive at the Walker equation, the ansatz in Equation 3.1 and Equation 3.2 is substituted into the Landau-Lifshitz equation (1.3). Including only terms of at least first order in either h_i or m_i (but not both) allows solving m_i in terms of h_i:

$$\begin{aligned} & i\omega(m_x, m_y, 0)e^{i\omega t} \\ =&\gamma(m_y H_0 - h_y M_0, h_x M_0 - m_x H_0, 0)e^{i\omega t} \\ \Rightarrow& \end{aligned} \tag{3.5}$$

$$4\pi m_x = \underbrace{\frac{4\pi\gamma^2 H_0 M_0}{\gamma^2 H_0^2 - \omega^2}}_{\kappa} h_x - i\underbrace{\frac{4\pi\gamma M_0\omega}{\gamma^2 H_0^2 - \omega^2}}_{\nu} h_y \tag{3.6}$$

$$4\pi m_y = i\nu h_x + \kappa h_y. \tag{3.7}$$

Substituting these into the Gauss law (2.1) gives, after cancelling some complex terms, the Walker equation inside the cylinder:

$$\begin{aligned} 0 =& \nabla^2 \Psi + 4\pi \nabla \cdot \vec{m} \\ =& \left[\underbrace{(1+\kappa)}_{\mu} \left(\frac{\partial^2}{\partial x^2} + \frac{\partial^2}{\partial y^2} \right) + \frac{\partial^2}{\partial z^2} \right] \Psi(\vec{r}) \\ =& \mu \left[\frac{\partial^2}{\partial r^2} + \frac{1}{r}\frac{\partial}{\partial r} + \frac{1}{r^2}\frac{\partial^2}{\partial \theta^2} \right] \Psi(\vec{r}) + \frac{\partial^2 \Psi(\vec{r})}{\partial z^2} \end{aligned} \tag{3.8}$$

Outside the cylinder, $\kappa = 0$ and we only need to solve the Laplace equation Equation 3.3.

3.2 BOUNDARY CONDITIONS

In general, continuous solutions of $\Psi(\vec{r})$ are preferred. Further, the resulting fields $\vec{h}$ and $\vec{b}$ should vanish eventually, i.e. as $|\vec{r}| \to \infty$. For a separable solution $\Psi(r,\theta,z) = R(r)\,\Theta(\theta)\,Z(z)$, the fields are proportional to either $R(r)\frac{\mathrm{d}Z(z)}{\mathrm{d}z}$ or $Z(z)\frac{\mathrm{d}R(r)}{\mathrm{d}r}$, so $R(r) \to^{r\to\infty} 0$ and $Z(z) \to^{z\to\infty} 0$, and in particular $\Psi(\vec{r})$ must also vanish at large enough distances.

Besides the vanishing and continuity conditions for Ψ, there are also Maxwell continuity conditions for $\vec{h}$ and $\vec{b}$: at the surface of the cylinder, the parallel component of $\vec{h}$ and the normal component of $\vec{b}$ must be continuous. As $b_z = h_z$ (as $m_z = 0$ by assumption), this implies that at the ends of the cylinder one must check both the parallel and the normal component of $\vec{h}$. In cylinder coordinates, the components of $\vec{h}$ are

$$\vec{h} = \nabla\Psi = \left(\frac{\partial\Psi}{\partial r}, \frac{1}{r}\frac{\partial\Psi}{\partial\theta}, \frac{\partial\Psi}{\partial z} \right).$$

From Equation 3.6 and Equation 3.7 we have that

$$\begin{aligned} 4\pi m_x &= \kappa\frac{\partial\Psi}{\partial x} - i\nu\frac{\partial\Psi}{\partial y} \\ 4\pi m_y &= i\nu\frac{\partial\Psi}{\partial x} + \kappa\frac{\partial\Psi}{\partial y}. \end{aligned}$$

Writing these in cylinder coordinates we obtain

$$4\pi m_r = \kappa\frac{\partial\Psi}{\partial r} - \frac{i\nu}{r}\frac{\partial\Psi}{\partial\theta} \tag{3.9}$$

$$4\pi m_\theta = i\nu\frac{\partial\Psi}{\partial r} + \frac{\kappa}{r}\frac{\partial\Psi}{\partial\theta}. \tag{3.10}$$

The components of $\vec{b}$ are then

$$\vec{b} = \nabla\Psi + 4\pi\vec{m} = \begin{cases} \left(\mu\frac{\partial\Psi}{\partial x} - i\nu\frac{\partial\Psi}{\partial y}, i\nu\frac{\partial\Psi}{\partial x} + \mu\frac{\partial\Psi}{\partial y}, \frac{\partial\Psi}{\partial z}\right) & \text{inside} \\ \left(\frac{\partial\Psi}{\partial x}, \frac{\partial\Psi}{\partial y}, \frac{\partial\Psi}{\partial z}\right) & \text{outside} \end{cases}$$
$$= \begin{cases} \left(\mu\frac{\partial\Psi}{\partial r} - \frac{i\nu}{r}\frac{\partial\Psi}{\partial\theta}, i\nu\frac{\partial\Psi}{\partial r} + \frac{\mu}{r}\frac{\partial\Psi}{\partial\theta}, \frac{\partial\Psi}{\partial z}\right) & \text{inside} \\ \left(\frac{\partial\Psi}{\partial r}, \frac{1}{r}\frac{\partial\Psi}{\partial\theta}, \frac{\partial\Psi}{\partial z}\right). & \text{outside} \end{cases}$$

At the ends of the cylinder the continuity of the parallel component of $\vec{h}$ needs to be checked, that is

$$\vec{h}\cdot(a\hat{\mathbf{e}}_r + b\hat{\mathbf{e}}_\theta) = \left(a\frac{\partial\Psi}{\partial r}, b\frac{1}{r}\frac{\partial\Psi}{\partial\theta}, 0\right), \quad a^2 + b^2 = 1.$$

The normal component of $\vec{b}$ is in this case $h_z = \frac{\partial\Psi}{\partial z}$, so its continuity is also a requirement. This boundary condition 'quantizes' the axial mode functions.

However, it turns out that the condition for the parallel component of $\vec{h}$ is redundant: at the ends, the continuity of Ψ and its separability together result in $\Psi^A(r,\theta,z_{\text{end}}) = \Psi^C(r,\theta,z_{\text{end}})$ in the disc where areas A and C intersect (see Figure 3.1 for the labels). Hence, all derivatives with respect to r and θ are equal.

On the sides of the cylinder, the continuity of the parallel component of $\vec{h}$ is

$$\vec{h}\cdot(a\vec{e_\theta} + b\vec{e_z}) = \left(0, a\frac{1}{r}\frac{\partial\Psi}{\partial\theta}, b\frac{\partial\Psi}{\partial z}\right), \quad a^2 + b^2 = 1.$$

As with the ends, this condition is also redundant for the same reason. The normal component of $\vec{b}$, however, is not trivial, and determines the radial mode functions:

$$\begin{aligned} \vec{b}_r &= \mu\frac{\partial\Psi^A}{\partial r} - \frac{i\nu}{r}\frac{\partial\Psi^A}{\partial\theta} = \frac{\partial\Psi^B}{\partial r} \\ &= \mu\frac{\partial\Psi^A}{\partial r} + \frac{l\nu}{r}\Psi^A = \frac{\partial\Psi^B}{\partial r}. \end{aligned} \tag{3.11}$$

In the literature of spin waves and magnetostatics the so-called pinning boundary conditions are used for various reasons. One important reason is simply that they are easier, as the outside of the container need not be considered. Generally, pinning boundary conditions imply either that the derivative or the function itself (or some combination thereof) is zero at the boundary, e.g.

$$\alpha\zeta + \beta\frac{\partial\zeta}{\partial w} = 0$$

so that α and β are not both zero. For spin pinning, the function $\zeta(w)$ is usually the magnetization, which either vanishes or reaches an extremum at the boundary. In our case it applies only to m_r, as $m_z = 0$ by assumption.

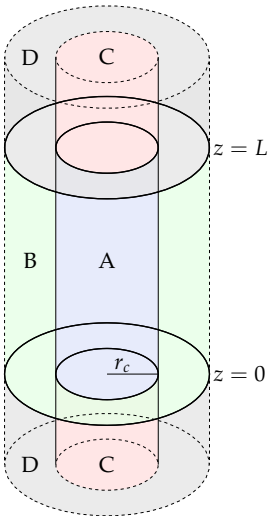

Figure 3.1: Areas of the Cylinder

3.3 SEPARABLE SOLUTIONS

The separable solutions outside the cylinder are solutions to the Laplace equation (3.3) in cylindrical coordinates (r, θ, z) obtained by the usual method of separation of variables, $\Psi(r, \theta, z) = R(r)\Theta(\theta)Z(z)$. From these we must choose those solutions which vanish at infinity, fulfill the condition that $\Psi(r, \theta + 2\pi, z) = \Psi(r, \theta, z)$ and are well-behaved when $r = 0$. In cylinder coordinates, the cylinder divides space into four different areas with distinct solutions. Given a cylinder of length L with ends at 0 and L, the first area (A) is the inside of the cylinder. The second area (B) is the outside of the cylinder between $z = 0$ and $z = L$. The areas outside $z \in [0, L]$ are likewise divided by $r = r_c$ into C ($r < r_c$) and D ($r > r_c$). This divide arises from the different r and z dependencies of the solutions.

Solutions outside the cylinder are cylindrical solutions to the Laplace equation with the following possibilities:

$$\Psi^{\text{out}}(r, \theta, z) = \begin{cases} J_l(mr) & e^{il\theta}\left(A\cosh(mz) + B\sinh(mz)\right) \\ Y_l(mr) & e^{il\theta}\left(A\cosh(mz) + B\sinh(mz)\right) \\ I_l(mr) & e^{il\theta}\left(A\cos(mz) + B\sin(mz)\right) \\ K_l(mr) & e^{il\theta}\left(A\cos(mz) + B\sin(mz)\right) \end{cases} \tag{3.12}$$

Here J_l, Y_l are Bessel functions of the first and second kind, respectively, and I_l, K_l the modified Bessel functions of the first and second kind, respectively. Symmetry dictates that $l \in \mathbb{Z}$, and in the case of $l = 0$ the solution $\Theta(\theta) = C \in \mathbb{C}$. For $m = 0$ the solution is

$$\Psi(r, \theta, z) = \left(Ar^l + Br^{-l}\right)(Cz + D)\, e^{il\theta}. \tag{3.13}$$

For $m = 0 = l$ the solution is

$$\Psi(r,\theta,z) = (A\ln(r) + B)(Cz + D). \tag{3.14}$$

Inside the cylinder when $\mu \neq 0$, the general solutions to Equation 3.8 are of the form

$$\Psi^{\text{in}}(\vec{r}) = \begin{cases} J_l(kr)\, e^{il\theta}\left(A^+ \cosh\left(k\sqrt{\mu}z\right) + B^+ \sinh\left(k\sqrt{\mu}z\right)\right) \\ I_l(kr)\, e^{il\theta}\left(A^+ \cos\left(k\sqrt{\mu}z\right) + B^+ \sin\left(k\sqrt{\mu}z\right)\right) \end{cases} \quad \mu > 0 \tag{3.15}$$

$$\Psi^{\text{in}}(\vec{r}) = \begin{cases} J_l(kr)\, e^{il\theta}\left(A^- \cos(k\sqrt{-\mu}z) + B^- \sin(k\sqrt{-\mu}z)\right) \\ I_l(kr)\, e^{il\theta}\left(A^- \cosh(k\sqrt{-\mu}z) + B^- \sinh(k\sqrt{-\mu}z)\right). \end{cases} \quad \mu < 0 \tag{3.16}$$

Other Bessel functions are also solutions but have a discontinuity at $r = 0$ and hence are not included. Alternatively, the $\sqrt{\pm\mu}$ may be moved from scaling z to scaling r (e.g. $J_l\left(\frac{kr}{\sqrt{\pm\mu}}\right)$). In the cases $k = 0$ and $k = 0 = l$, the solutions are the same as outside the cylinder, or one may rescale the solutions with $(\pm\mu)^{-\frac{1}{2}}$ as in the previous case without affecting the results.

If $\mu = 0$, equation Equation 3.8 reduces to $\frac{\partial^2\Psi(\vec{r})}{\partial z^2} = 0$, for which the solutions are

$$\Psi(r,\theta,z) = A(r,\theta)z + B(r,\theta), \tag{3.17}$$

and the associated frequency

$$\omega = |\gamma| H_0 \sqrt{1 + \frac{4\pi M}{H_0}}.$$

3.4 SOLUTION FOR $\mu < 0$

For an infinite cylinder, the solutions have been considered in [18]; the solutions for a finite cylinder are similar with a few notable differences (as we shall demonstrate): (1) one has to account for the demagnetizing field, (2) the solutions are not entirely separable, (3) the separation constant in z-direction becomes discrete, and (4) the so-called surface solutions (for $\mu > 0$) vanish.

The problem with separability arises because the solutions cannot be exactly matched over all four areas A, B, C and D. This can be seen as follows:

In area C outside the cylinders, the solutions can be of only one form:

$$\Psi^C = \begin{cases} A_< J_{n_<}(m_< r) e^{in_<\theta} e^{m_< z} & z < 0 \\ A_> J_{n_>}(m_> r) e^{in_>\theta} e^{-m_> z} & z > L \end{cases}$$

This is due to the requirement that Ψ be continuous at $r = 0$ ($\Rightarrow J_n$) and that Ψ vanish far away from the cylinder, including as $z \to \infty$, which forces the exponential z-dependence; $\Psi^C = 0$ is ruled out by boundary conditions, as they would otherwise force Ψ to be zero everywhere.

As $\Psi^A(r,\theta,L) = \Psi^C(r,\theta,L)$, it follows that the r-dependence must be the same in both areas. Using similar arguments the r-dependence must also be the same in B and D, and the z-dependence must be same in A and B as well as C and D. However, for $\mu < 0$ all these conditions cannot hold simultaneously: by Equation 3.16, the AC boundary forces the z-dependence to be sinusoidal in A, which at the AB boundary forces the r-dependence in C to be $K_n(mr)$ (see Equation 3.12), whence it follows from applying BD boundary conditions that z-dependence in D be sinusoidal (by Equation 3.12), while the CD boundary demands that it be exponentially decaying.

From this analysis it is clear that these solutions are not truly separable. However, judging from the cases of the infinite disc and the infinite cylinder, it may be that the problematic area is the area D alone, and it may be that ignoring it altogether will not affect the frequency spectrum of the solutions obtained simply by matching the boundaries AB and AC. Thus the solutions have the following the form:

$$\Psi(r,\theta,z) = \begin{cases} J_l(kr)\, e^{il\theta}\left(A^- \cos(k\sqrt{-\mu}z) + B^- \sin(k\sqrt{-\mu}z)\right) & \text{in A} \\ \begin{cases} A_< J_{n_<}(m_< r) e^{in_<\theta} e^{m_< z} & z < 0 \\ A_> J_{n_>}(m_> r) e^{in_>\theta} e^{-m_> z} & z > L \end{cases} & \text{in C} \\ K_n(mr) e^{in\theta}\left(A^{\text{out}} \cos(mz) + B^{\text{out}} \sin(mz)\right). & \text{in B} \end{cases}$$

Continuity conditions for Ψ give

$$\begin{cases} J_l(kr)\, e^{il\theta} A^- = A_< J_{n_<}(m_< r) e^{in_<\theta} & z = 0 \\ \begin{cases} J_l(kr)\, e^{il\theta}\left(A^- \cos(k\sqrt{-\mu}L) + B^- \sin(k\sqrt{-\mu}L)\right) \\ = A_> J_{n_>}(m_> r) e^{in_>\theta} e^{-m_> L} \end{cases} & z = L \\ \begin{cases} J_l(kr_c)\, e^{il\theta}\left(A^- \cos(k\sqrt{-\mu}z) + B^- \sin(k\sqrt{-\mu}z)\right) \\ = K_n(mr_c) e^{in\theta}\left(A^{\text{out}} \cos(mz) + B^{\text{out}} \sin(mz)\right). \end{cases} & r = r_c \end{cases} \tag{3.18}$$

It follows that

$$
\begin{aligned}
l = n = n_> = n_< \\
k = m_< = m_> \\
m = k\sqrt{-\mu} \\
A^- = A_< \\
cA^- = A^{\text{out}} \\
cB^- = B^{\text{out}},
\end{aligned}
$$

where $c = \frac{J_l(kr_c)}{K_l(k\sqrt{-\mu}r_c)}$. The continuity condition for the normal component of $\vec{h}$ gives

$$
\begin{cases}
B^-\sqrt{-\mu} = A_< & z = 0 \\
\sqrt{-\mu}\left(B^-\cos(k\sqrt{-\mu}L) - A^-\sin(k\sqrt{-\mu}L)\right) = -A_> e^{-kL} & z = L.
\end{cases}
\tag{3.19}
$$

Combining this with previous results from Equation 3.18 results in the solutions:

$$
\Psi(r,\theta,z) = \begin{cases}
B^- J_l(kr)\, e^{il\theta}\left(\sqrt{-\mu}\cos(k\sqrt{-\mu}z) + \sin(k\sqrt{-\mu}z)\right) & \text{in A} \\
\begin{cases}
B^-\sqrt{-\mu}J_l(kr)e^{il\theta}e^{kz} & z < 0 \\
\left(\frac{1}{2}B^-(1-\mu)\sin(k\sqrt{-\mu}L)e^{kL}\right) J_l(kr)e^{il\theta}e^{-kz} & z > L
\end{cases} & \text{in C} \\
\left(B^- \frac{J_l(kr_c)}{K_l(k\sqrt{-\mu}r_c)}\right) K_l(k\sqrt{-\mu}r)e^{il\theta}\left(\sqrt{-\mu}\cos(k\sqrt{-\mu}z) + \sin(k\sqrt{-\mu}z)\right) & \text{in B.}
\end{cases}
$$

In particular, the factor of $\frac{1}{2}$ in the $z > L$ in area C is obtained by subtracting the $z = L$ of Equation 3.19 from that of Equation 3.18.

$$
\frac{\partial\Psi(\vec{r})}{\partial r} = \begin{cases}
B^- \frac{J_{l-1}(kr) - J_{l+1}(kr)}{2} k e^{il\theta}\left(\sqrt{-\mu}\cos(k\sqrt{-\mu}z) + \sin(k\sqrt{-\mu}z)\right) & \text{in A} \\
\begin{cases}
B^-\sqrt{-\mu}\frac{J_{l-1}(kr) - J_{l+1}(kr)}{2} k e^{il\theta}e^{kz} & z < 0 \\
\left(\frac{1}{2}B^-(1-\mu)\sin(k\sqrt{-\mu}L)e^{kL}\right)\frac{J_{l-1}(kr) - J_{l+1}(kr)}{2} k e^{il\theta}e^{-kz} & z > L
\end{cases} & \text{in C} \\
\begin{cases}
\left(B^- \frac{J_l(kr_c)}{K_l(k\sqrt{-\mu}r_c)}\right)\frac{K_{l+1}(k\sqrt{-\mu}r) + K_{l-1}(k\sqrt{-\mu}r)}{-2} \\
\quad \times k\sqrt{-\mu}e^{il\theta}\left(\sqrt{-\mu}\cos(k\sqrt{-\mu}z) + \sin(k\sqrt{-\mu}z)\right)
\end{cases} & \text{in B}
\end{cases}
$$

$$
\frac{1}{r}\frac{\partial\Psi(\vec{r})}{\partial\theta} = \begin{cases}
B^- J_l(kr)\,\frac{ile^{il\theta}}{r}\left(\sqrt{-\mu}\cos(k\sqrt{-\mu}z) + \sin(k\sqrt{-\mu}z)\right) & \text{in A} \\
\begin{cases}
B^-\sqrt{-\mu}J_l(kr)\frac{ile^{il\theta}}{r}e^{kz} & z < 0 \\
\left(\frac{1}{2}B^-(1-\mu)\sin(k\sqrt{-\mu}L)e^{kL}\right) J_l(kr)\frac{ile^{il\theta}}{r}e^{-kz} & z > L
\end{cases} & \text{in C} \\
\begin{cases}
\left(B^- \frac{J_l(kr_c)}{K_l(k\sqrt{-\mu}r_c)}\right) K_l(k\sqrt{-\mu}r)(-l)\frac{ile^{il\theta}}{r} \\
\quad \times\left(\sqrt{-\mu}\cos(k\sqrt{-\mu}z) + \sin(k\sqrt{-\mu}z)\right)
\end{cases} & \text{in B}
\end{cases}
$$

$$\frac{\partial\Psi(\vec{r})}{\partial z} = \begin{cases} B^- J_l(kr)\, e^{il\theta}\left(\cos(k\sqrt{-\mu}z) - \sqrt{-\mu}\sin(k\sqrt{-\mu}z)\right) k\sqrt{-\mu} & \text{in A} \\ \begin{cases} B^-\sqrt{-\mu}J_l(kr)e^{il\theta}ke^{kz} & z<0 \\ \left(\frac{1}{2}B^-(1-\mu)\sin(k\sqrt{-\mu}L)e^{kL}\right) J_l(kr)e^{il\theta}(-k)e^{-kz} & z>L \end{cases} & \text{in C} \\ \begin{cases} \left(B^- \frac{J_l(kr_c)}{K_l(k\sqrt{-\mu}r_c)}\right) K_l(k\sqrt{-\mu}r)e^{il\theta} \\ \times\left(\cos(k\sqrt{-\mu}z) - \sqrt{-\mu}\sin(k\sqrt{-\mu}z)\right) k\sqrt{-\mu} \end{cases} & \text{in B.} \end{cases}$$

The equations also impose a condition (dispersion relation) for k:

$$\begin{aligned} \tan\left(k\sqrt{-\mu}L\right) =& \frac{-2\sqrt{-\mu}}{1+\mu} \\ \Leftrightarrow & \\ k =& \frac{1}{\sqrt{-\mu}L}\left[\arctan\left(\frac{-2\sqrt{-\mu}}{1+\mu}\right) + n\pi\right],\ n\in\mathbb{N}. \end{aligned} \tag{3.20}$$

For k to remain positive (i.e., decaying solutions), n may only take non-negative values.

The continuity for $\vec{b}_r$, from Equation 3.11, gives the characteristic equation

$$\begin{aligned} & \mu k J_l'(kr_c) + \frac{l\nu}{r_c} J_l(kr_c) \\ =& \frac{J_l(kr_c)}{K_l(k\sqrt{-\mu}r_c)} K_l'(k\sqrt{-\mu}r_c) k\sqrt{-\mu} \\ \Leftrightarrow\ 0 =& \mu k J_l'(kr_c) + J_l(kr_c) \\ & \times\left(\frac{l\nu}{r_c} - \frac{K_l'(k\sqrt{-\mu}r_c)}{K_l(k\sqrt{-\mu}r_c)} k\sqrt{-\mu}\right) \\ & \Leftrightarrow \frac{\mu k J_l'(kr_c)}{J_l(kr_c)} + \frac{l\nu}{r_c} \\ =& \frac{K_l'(k\sqrt{-\mu}r_c) k\sqrt{-\mu}}{K_l(k\sqrt{-\mu}r_c)} \\ \Leftrightarrow & \frac{\frac{1}{2}\mu k\left(J_{l-1}(kr_c) - J_{l+1}(kr_c)\right)}{J_l(kr_c)} + \frac{l\nu}{r_c} \\ =& \frac{-\frac{1}{2}k\sqrt{-\mu}\left(K_{l-1}(k\sqrt{-\mu}r_c) + K_{l+1}(k\sqrt{-\mu}r_c)\right)}{K_l(k\sqrt{-\mu}r_c)} \end{aligned}$$

$$\therefore J_l(kr_c)K_l'(k\sqrt{-\mu}r_c)k\sqrt{-\mu} - K_l(k\sqrt{-\mu}r_c)\left[\mu k J_l'(kr_c) + \frac{l\nu}{r_c}J_l(kr_c)\right] = 0. \tag{3.21}$$

The form of the characteristic equation is equivalent to that derived in [18]; the minute differences are accounted for by the choice of

the place of μ in the solutions Equation 3.16 (whether it scales the z-solution or the r-solution). However, in evaluating the solutions to Equation 3.21, one must also account for Equation 3.20.

3.5 THE CHARACTERISTIC EQUATION

The characteristic equation has solutions for $\mu < 0$. Introducing the scaled frequency $\widetilde{\omega} \equiv \frac{\omega}{\gamma H_0}$ and defining $\Omega_H \equiv \frac{4\pi M}{H_0}$, $\Omega_0 = \sqrt{1+\Omega_H}$ we may express μ and ν as

$$\begin{aligned} \mu &= \frac{\Omega_0^2 - \widetilde{\omega}^2}{1-\widetilde{\omega}^2} \\ \nu &= \frac{\frac{1}{\Omega_H}\widetilde{\omega}}{1-\widetilde{\omega}^2}. \end{aligned} \tag{3.22}$$

Solutions exist when the scaled frequency is in the range $[1, \Omega_0]$, so $\mu \in [-\infty, 0]$ and $\nu \in [-\infty, \Omega_0]$. For numerical evaluation, Equation 3.20 may be substituted into Equation 3.21; the derivatives of Bessel functions may also be replaced using the identities for Bessel functions:

$$\begin{aligned} &\frac{1}{2}\mu k \left(J_{l-1}(kr_c) - J_{l+1}(kr_c)\right) + J_l(kr_c) \\ &\qquad \times \left(\frac{l\nu}{r_c} + \frac{K_{l-1}(k\sqrt{-\mu}r_c) + K_{l+1}(k\sqrt{-\mu}r_c)}{2K_l(k\sqrt{-\mu}r_c)} k\sqrt{-\mu}\right) = 0. \end{aligned}$$

The dispersion relation Equation 3.20 has a discontinuity at $\mu = -1$ or $\widetilde{\omega} = \sqrt{\frac{\Omega_0^2+1}{2}}$, which results in a change of branch of the arctan function. Hence, for a given n, k should be given as

$$k = \begin{cases} \frac{1}{\sqrt{-\mu}L}\left[\tan^{-1}\left(\frac{-2\sqrt{-\mu}}{1+\mu}\right) + n\pi\right] & \widetilde{\omega} < \sqrt{\frac{\Omega_0^2+1}{2}} \\ \frac{1}{\sqrt{-\mu}L}\left[\tan^{-1}\left(\frac{-2\sqrt{-\mu}}{1+\mu}\right) + (n+1)\pi\right] & \widetilde{\omega} > \sqrt{\frac{\Omega_0^2+1}{2}}. \end{cases}$$

3.5.1 *Approximations of Mode Frequencies*

To study the solutions, it is convenient to parametrize $-\mu = \cot^2 s$, $s \in [0, \frac{\pi}{2}]$. Thus the right-hand side of Equation 3.20 becomes $\tan 2s$ and the expression for k reduces to

$$k = \frac{n\pi + 2s}{L\cot s}. \tag{3.23}$$

This expression has no discontinuity. It is also clear that we must have $n \geq 0$ for $k > 0$ when $s \in [0, \frac{\pi}{2}]$. Solving ν as a function of μ and substituting $-\mu = \cot^2 s$ gives

$$\nu = -\sqrt{(\Omega_0^2 - \mu)(1-\mu)} = -\left(\Omega_H + \csc^2 s\right)^{\frac{1}{2}} \csc s.$$

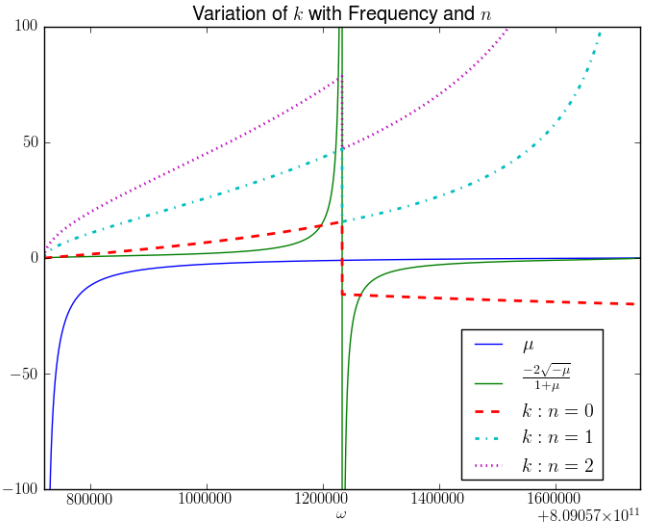

Figure 3.2: k as a Function of ω

The characteristic equation becomes

$$-\frac{n\pi+2s}{L}\cot s\, J_l'\left(\frac{n\pi+2s}{L\cot s}r_c\right)+J_l\left(\frac{n\pi+2s}{L\cot s}r_c\right)$$
$$\times\left(-\frac{l}{r_c}\left(\Omega_H+\csc^2 s\right)^{\frac{1}{2}}\csc s+\frac{K_l'(\frac{n\pi+2s}{L}r_c)}{K_l(\frac{n\pi+2s}{L}r_c)}\frac{n\pi+2s}{L}\right)=0.$$

The equation contains two terms, one multplied by the Bessel functions J_l and one by its derivative J_l'. Approximate solutions for the equation may be found when one dominates. When the first term dominates, the approximate solutions are given by

$$\frac{n\pi+2s}{L\cot s}r_c=j_{lm}'. \tag{3.24}$$

Here j_{lm}' denotes the roots of the first derivatives of J_l enumerated by $m=0,1,2...$ When the second term dominates, the solutions are obtained by replacing j_{lm}' by j_{lm}, the zeros of the Bessel function of order l. Equation 3.24 is transcendental and hence has to be solved numerically. Approximations can be found for $s\approx 0$ and $s\approx\frac{\pi}{2}$:

$$\begin{aligned}\frac{n\pi+2s}{Lj_{lm}}r_c &= \begin{cases}\cot s\approx\frac{1}{s} & s\approx 0\\ \cot\left(\frac{\pi}{2}-\left(\frac{\pi}{2}-s\right)\right)=\tan\left(\frac{\pi}{2}-s\right)\approx\left(\frac{\pi}{2}-s\right) & s\approx\frac{\pi}{2}\end{cases}\\ s &= \begin{cases}\frac{n\pi}{4}\left(\sqrt{1+\frac{8Lj_{lr}}{n^2\pi^2 d}}-1\right)\approx\frac{Lj_{ml}}{n\pi r_c} & s\approx 0\\ \frac{\pi}{2}\frac{Lj_{lm}-n(2r_c)}{Lj_{lm}+2r_c} & s\approx\frac{\pi}{2}.\end{cases}\end{aligned} \tag{3.25}$$

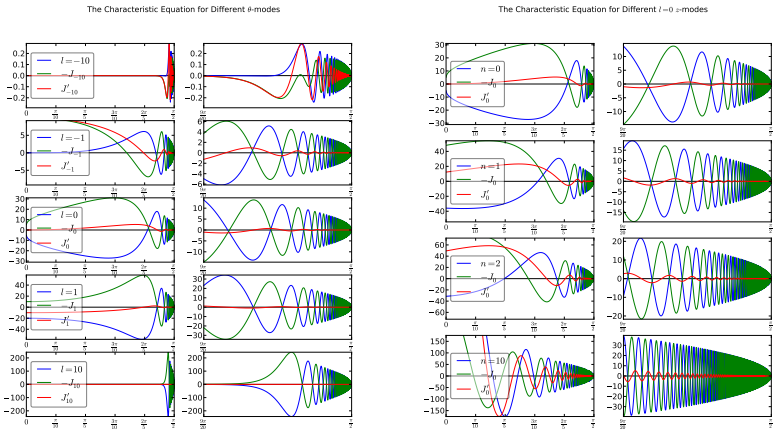

Figure 3.3: The Characteristic Equation

Comparison of the characteristic equation with the J_l and J_l' terms. Simulation parameters are $L = 0.10\text{cm}$, $\rho = 2 \cdot 10^{17}\text{cm}^{-3}$, $H = 4.6 \cdot 10^4\text{Oe} = 4.6\text{T}$.

Evidently the $s \approx 0$ works best for large n. $s \approx \frac{\pi}{2}$, on the other hand, requires either a large r or a small n to remain positive. Whether j_{lm} or j'_{lm} should be used in the above expressions is more complicated. For sufficiently large s, the J_l term will always dominate since $\cot s$ in the J_l' (prime) term takes the whole term to zero. As l increases, the roots of the characteristic equation shift towards $s \approx \frac{\pi}{2}$, as can be seen in Figure 3.3; it also illustrates the coincidence of roots of the J_l term and the characteristic equation for large s. The oscillation of the function increases with s to squeeze the numerable set of roots of the Bessel function into a finite interval, and so the modes get denser as s approaches the uniform precession frequency at $s = \frac{\pi}{2}$, which is an accumulation point of the modes.

A larger n increases the magnitude of the arguments of the Bessel functions. Consequently, the zeros of J_l and J_l' occur at smaller values of s. This increases the scaling effect of $\cot s$ factor of the primed term; it should dominate for small s. Figure 3.3 illustrates the increasing discrepancy between the J_l term and the characteristic equation for small s and the increasing coherence with J_l'. However, with large s the characteristic equation once again approaches the oscillating J_l term to a high degree.

As $-\mu = \cot^2 s$, it is convenient to solve $\widetilde{\omega}$ as a function of s. From Equation 3.22,

$$\widetilde{\omega}^2 = \frac{\Omega_0^2 + \cot^2 s}{1 + \cot^2 s} = \Omega_H \sin^2 s + 1.$$

When $M_0 \ll H_0$, or for small s,

$$\widetilde{\omega} = \sqrt{1 + \Omega_H \sin^2 s} \approx 1 + \frac{\Omega_H}{2} \sin^2 s.$$

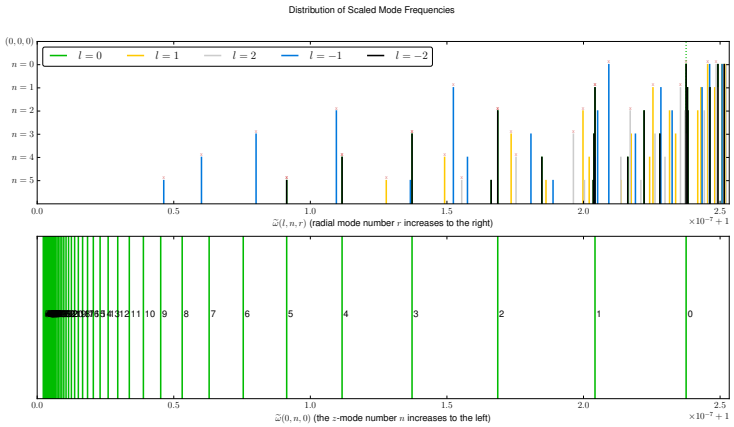

Figure 3.4: Frequency Distribution for Some Modes

$L = 0.10\text{cm}$, $\rho = 2 \cdot 10^{17}\text{cm}^{-3}$, $H = 4.6 \cdot 10^4\text{Oe} = 4.6\text{T}$. Modes $(0,3,0)$,$(-1,0,0)$,$(-2,0,0)$,$(-3,0,0)$,$(-3,0,1)$,$(-4,0,0)$,$(-5,0,0)$, and$(-5,0,1)$ near $\widetilde{\omega} = 1$ are indistinguishable from the upper picture.

For atomic hydrogen,

$$\omega \approx |\gamma| H_0 \left(1 + \frac{2\pi\mu_B\rho}{H_0} \sin^2 s\right),$$

where s is given by one of the equations in Equation 3.25.

3.6 MODE DISTRIBUTION

As can be seen from e.g. Equation 3.25, three numbers are needed to specify the solution: the azimuthal (θ) number $l \in \mathbb{Z}$, the axial (z) number $n \in \mathbb{N} \cup \{0\}$, and the radial number $m \in \mathbb{N} \cup \{0\}$ (grouped as the triple (l,n,m)). Contrary to [6], who used pinning boundary conditions, the azimuthal l and $-l$ modes are not degenerate owing to the characteristic equation Equation 3.21, which arises from the radial boundary condition.

As is already clear from Figure 3.3 and Figure 3.3, the mode frequencies accumulate up (to the right) to the uniform precession frequency $\widetilde{\omega} \approx \Omega_0 = \sqrt{1 + \Omega_H}$. However, the modes for which axial n is large compared to l and m, the mode frequencies approach $\widetilde{\omega} = 1$ (that is, γH_0), as is evident from Figure 3.4. For higher m the frequencies again move up towards Ω_0.

In conclusion, the modes appear to be very dense in the frequency domain $[1, \Omega_0]$, even for a given l, owing to the fact that higher n modes acculumate down and higher m modes up.

Part III

CONCLUSIONS

4 DISCUSSION

Similarly to [21], an infinite number of modes were found in the interval $\omega \in \left(|\gamma_e|\,\mu_0 H_0, |\gamma_e|\,\mu_0\sqrt{H_0 B_0}\right)$ for which $\mu < 0$. In contrast, however, the modes were also quantized in the axial direction owing to an additional axial boundary condition (as one might expect). Both limits of the interval appear to be accumulation points of mode frequencies: the upper limits for radial and azimuthal ($|l| \to \infty$) modes, the lower limit for axial modes.

Somewhat surprisingly no modes were found below this interval, contrary to the infinite cylinder[21]. These modes correspond to the $\mu > 0$ solutions (section A.3). As our treatment essentially amounts to putting boundary conditions in the axial direction, it is easy to lay blame on them for the missing modes. Mathematically, the continuity boundary condition in the z-direction makes the characteristic equation unsolvable: the inside of the cylinder requires some sort of exponential solution e^{kz}, which cannot be connected to a (separable) vanishing solution $Z(z) \overset{|z|\to\infty}{\longrightarrow} 0$ through the boundary. For a pinning boundary condition (section 3.2) it is likely such modes will exist, though there is no obvious physical justification for using them.

Although mathematically it is easy to blame the boundary conditions, it must be also taken into account that the physical nature of the problem changes qualitatively as the cylinder becomes finite: the demagnetizing field becomes non-uniform. Indeed, the shape of the demagnetizing field may lend some support to using some kind of pinning boundary conditions to model the problem as the next step; however, a distintictly better approach would be to simply account for the non-uniform demagnetizing field, for example using the generalized Walker equation[3]. Unfortunately this is far from trivial analytically, though perhaps more tractable computationally.[1]

Given all this careful theoretical work, the question of whether these modes are observed in the actual experiment begs for an answer. The generalized magnetostatic equation is expected to have wavelike solutions in the frequency range [3]

$$\gamma H(\vec{r}) < \omega < \gamma\sqrt{H(\vec{r})B(\vec{r})},$$

which evaluates to $\Delta\omega \sim 6 - 60\,\mathrm{mG}$, placing the modes on top of our main peak. So it is possible that the modes are excited and modify the main peak; however, the resolution of the setup is not expected to

1 Some simulations were attempted with the FlexPDE software, but unfortunately they were not very informative.

be sufficient to detect them. For a more thorough comparison with experiment, see [26] for details.

Part IV

APPENDIX

A

APPENDIX

A.1 A NOTE ON LINEARITY OF THE WALKER EQUATION

As an eigenvalue equation, Walker's equation is not linear. In general, a solution is determined by the pair (Ψ_i, μ_i) (possibly degenerate), but $c_1\Psi_1 + c_2\Psi_2$ is not a solution:

$$\begin{aligned}\partial_z^2 (c_1\Psi_1 + c_2\Psi_2) =& c_1\partial_z^2\Psi_1 + c_2\partial_z^2\Psi_2 \\ =& c_1\left(-\mu_1\nabla_\perp^2\Psi_1\right) + c_2\left(-\mu_2\nabla_\perp^2\Psi_2\right) \\ =& -\mu_1\nabla_\perp^2 c_1\Psi_1 - \mu_2\nabla_\perp^2 c_2\Psi_2.\end{aligned}$$

$\nabla_\perp^2 = \partial_x^2 + \partial_y^2$

A linear combination is only a solution if the solutions are degenerate, i.e. $\mu_1 = \mu_2$. A similar thing happens with the time-independent Schrödinger equation, which is not linear either. However, the time-dependent Schrödinger equation is linear, as the time derivative absorbs the eigenvalue. The same does not occur in the case of the Walker equation, but it does occur for the linearized Landau-Lifshitz equation with proper definitions of quantities: namely, the solution produces the magnetization $(m_x, m_y, 0)$ – not (m_x, m_y, M_0) – and the related magnetic field h. Then a solution $c_1\Psi_1 + c_2\Psi_2$ produces $c_1\vec{m}_1 + c_2\vec{m}_2$ and $c_1\vec{h}_1 + c_2\vec{h}_2$ which are solutions of the Landau-Lifshitz equation. This can be seen by substituting the linear combination into the Landau-Lifshitz equation. The result is the following pair of equations:

$$\begin{aligned}ic_1 m_x\omega_1 e^{i\omega_1 t} + ic_2 m_x^2\omega_2 e^{i\omega_2 t} =& -H_0 c_1\gamma m_y^1 e^{i\omega_1 t} - H_0 c_2\gamma m_y^2 e^{i\omega_2 t} \\ &+M_0 c_1\gamma h_y^1 e^{i\omega_1 t} + M_0 c_2\gamma h_y^2 e^{i\omega_2 t} \\ ic_1 m_y\omega_1 e^{i\omega_1 t} + ic_2 m_y^2\omega_2 e^{i\omega_2 t} =& +H_0 c_1\gamma m_x^1 e^{i\omega_1 t} + H_0 c_2\gamma m_x^2 e^{i\omega_2 t} \\ &-M_0 c_1\gamma h_x^1 e^{i\omega_1 t} - M_0 c_2\gamma h_x^2 e^{i\omega_2 t}.\end{aligned}$$

With some rearrangement, the equations become

$$\begin{aligned}0 =& c_1\left(H_0\gamma m_y^1 e^{i\omega_1 t} - M_0\gamma h_y^1 e^{i\omega_1 t} + im_x^1\omega_1 e^{i\omega_1 t}\right) \\ &+c_2\left(H_0\gamma m_y^2 e^{i\omega_2 t} - M_0\gamma h_y^2 e^{i\omega_2 t} + im_x^2\omega_2 e^{i\omega_2 t}\right) \\ 0 =& c_1\left(-H_0\gamma m_x^1 e^{i\omega_1 t} + M_0\gamma h_x^1 e^{i\omega_1 t} + im_y^1\omega_1 e^{i\omega_1 t}\right) \\ &+c_2\left(-H_0\gamma m_x^2 e^{i\omega_2 t} + M_0\gamma h_x^2 e^{i\omega_2 t} + im_y^2\omega_2 e^{i\omega_2 t}\right).\end{aligned}$$

If the linear combination is to be a solution as well, then the above equalities must hold. The case looks promising as the expressions

multiplying c_1 contain only quantities with index 1 and similarly for c_2, so there is hope that the expressions vanish — and that is indeed what happens. Solving m_x^1 and m_y^1 from the pair of equations multiplying c_1 results in Equation 3.6 and Equation 3.7 which, with some manipulation, gives the Walker equation which is satisfied because $\vec{m}_1$ ($= \Psi_1$) is its solution. Hence a linear combination of solutions Ψ_1 and Ψ_2 solves the Landau-Lifshitz equation, so building series solutions to the equation is a legitimate effort.

A.2 SOLUTIONS FOR $\mu = 0$

In area C, the solution must be both well-behaved at $r = 0$ and vanish when $z \to \infty$. The only solution in (3.12) fulfilling both conditions is the one with J_n. Thus, in area C, the solutions are

$$\Psi^C = \begin{cases} A_< J_{n_<}(m_< r) e^{in_<\theta} e^{m_< z} & z < 0 \\ A_> J_{n_>}(m_> r) e^{in_>\theta} e^{-m_> z} & z > L \end{cases}$$

The first boundary conditions comes from the AC boundary when $z = 0$ and $z = L$ from the continuity of Ψ and its z-derivative. From (3.17) $\Psi_A(r,\theta,z) = A(r,\theta)z + B(r,\theta)$, and we see that the solutions must satisfy

$$\begin{aligned} B(r,\theta) &= A_< J_{n_<}(m_< r) e^{in_<\theta} && \text{(A.1)} \\ A(r,\theta)L + B(r,\theta) &= A_> J_{n_>}(m_> r) e^{in_>\theta} e^{-m_> L} && \text{(A.2)} \\ A(r,\theta) &= A_< m_< J_{n_<}(m_< r) e^{in_<\theta} && \text{(A.3)} \\ A(r,\theta) &= A_>(-m_>) J_{n_>}(m_> r) e^{in_>\theta} e^{-m_> L}. && \text{(A.4)} \end{aligned}$$

If $A(r,\theta) \neq 0$, dividing (A.3) by (A.4) gives

$$\frac{\text{(A.3)}}{\text{(A.4)}} = 1 = \frac{A_< m_< J_{n_<}(m_< r) e^{in_<\theta}}{A_>(-m_>) J_{n_>}(m_> r) e^{in_>\theta} e^{-m_> L}}$$

Hence, for the solution to fulfill both derivative conditions implies that $m_< = m_> \equiv m$, $n_< = n_> \equiv n$.[1]

$$\begin{aligned} \Rightarrow \quad 1 &= \frac{A_<}{-A_> e^{-mL}} \\ A_< &= -A_> e^{-mL} \equiv -A e^{-mL} \end{aligned}$$

The total solution can now be read from (A.3) and (A.1):

1 Because $J_n(-x) = (-1)^n J_n(x)$, in principle also $m_< = -m_>$ is a possibility; however, this would make the exponent function outside the cylinder diverge at one side.

$$
\begin{aligned}
(\text{A.4}) = A(r,\theta) &= A(-m)J_n(mr)e^{in\theta}e^{-mL} \\
(\text{A.1}) = B(r,\theta) &= A_< J_n(mr)e^{in\theta} \\
&= -AJ_n(mr)e^{in\theta}e^{-mL} \\
&= \frac{A(r,\theta)}{m} \\
\Rightarrow A(r,\theta) &= mB(r,\theta)
\end{aligned}
$$

$$
\begin{aligned}
\Psi^A &= A(r,\theta)\,z + B(r,\theta) \\
&= B(r,\theta)\,(mz+1) \\
&= -A(mz+1)\,J_n(mr)e^{in\theta}e^{-mL}
\end{aligned}
$$

The final boundary condition gives a value for m:

$$
\begin{aligned}
\Psi^A(z=L) &= -A(mL+1)\,J_n(mr)e^{in\theta}e^{-mL} \\
&\overset{(\text{A.2})}{=} A_> J_{n_>}(m_> r)e^{in_>\theta}e^{-m_> L} \\
&= AJ_n(mr)e^{in\theta}e^{-mL} \\
\Rightarrow mL+1 &= -1 \\
m &= -\frac{2}{L}.
\end{aligned}
$$

Finally,

$$
\begin{aligned}
\Psi^A &= -A\left(1-\frac{2z}{L}\right)J_n\left(-\frac{2r}{L}\right)e^{in\theta}e^2 \\
&= (-1)^n A\left(\frac{2z}{L}-1\right)J_n\left(\frac{2r}{L}\right)e^{in\theta}e^2 \\
\Psi^C &= \begin{cases} -A(-1)^n J_n\left(\frac{2r}{L}\right)e^{in\theta}e^{-\frac{2(z-L)}{L}} & z<0 \\ A(-1)^n J_n\left(\frac{2r}{L}\right)e^{in\theta}e^{\frac{2z}{L}} & z>L. \end{cases}
\end{aligned}
$$

This cannot be a solution, however, as Ψ_C does not vanish as $|z| \to \infty$: for $z > L$ the solution contains a factor of $e^{\frac{2z}{L}}$, which is not bounded. The same thing happens for $z < 0$. So solutions of this kind cannot exist for finite L; in the limit $L \to \infty$ there is no problem.

It could be that $A(r,\theta) = 0$. From (A.3) and (A.4) it follows that either $A_< = 0$ or $m_< = 0$ and $A_> = 0$ or $m_> = 0$. If either $m_<$ or $m_>$is zero, then the solution doesn't vanish as $|z| \to \infty$ unless the corresponding A is also zero. However, if one of the As is zero, it follows from (A.1) and (A.2) that the solution must be zero. Hence zero is the only possible solution for $\mu = 0$.

A.3 SOLUTIONS FOR $\mu > 0$

The Walker equation ostensibly admits a fully separable solution in the case of positive μ.

$$\Psi(r,\theta,z) = \begin{cases} J_l(kr)\, e^{\imath l\theta}\left(A^+\cosh\left(k\sqrt{\mu}z\right) + B^+\sinh\left(k\sqrt{\mu}z\right)\right) & \text{in A} \\ \begin{cases} A^C_< J_{n_<}(m^C_< r) e^{\imath n^C_< \theta} e^{m^C_< z} & z < 0 \\ A^C_> J_{n_>}(m^C_> r) e^{\imath n^C_> \theta} e^{-m^C_> z} & z > L \end{cases} & \text{in C} \\ J_n(mr) e^{\imath n\theta}\left(A^B\cosh(mz) + B^B\sinh(mz)\right) & \text{in B} \\ \begin{cases} A^D_< J_{n_<}(m^D_< r) e^{\imath n^D_< \theta} e^{m^D_< z} & z < 0 \\ A^D_> J_{n_>}(m^D_> r) e^{\imath n^D_> \theta} e^{-m^D_> z} & z > L \end{cases} & \text{in D} \end{cases}$$

Continuity conditions give $m = k\sqrt{\mu}$, $k = m^C_> = m^C_< = m^D_< = m^D_>$, $l = n = n^D_> = n^D_< = n^C_> = n^C_<$, $A^+ = A^C_<$, $A^B = A^D_<$ and

$$\begin{aligned} A^C_> e^{-kL} &= \left(A^+\cosh(k\sqrt{\mu}L) + B^+\sinh(k\sqrt{\mu}L)\right) \\ A^D_> e^{-kL} &= \left(A^B\cosh(k\sqrt{\mu}L) + B^B\sinh(k\sqrt{\mu}L)\right) \\ \frac{J_l(kr_c)}{J_n(k\sqrt{\mu}r)} &= c = \frac{\left(A^B\cosh\left(k\sqrt{\mu}z\right) + B^B\sinh\left(k\sqrt{\mu}z\right)\right)}{\left(A^+\cosh\left(k\sqrt{\mu}z\right) + B^+\sinh\left(k\sqrt{\mu}z\right)\right)} \\ &\Leftrightarrow \quad cA^+ = A^B, cB^+ = B^B \end{aligned}$$

$$\begin{aligned} B^+\sqrt{\mu} &= A^C_< = A^+ \\ B^B\sqrt{\mu} &= A^D_< = A^B \\ -A^C_> e^{-kL} &= \sqrt{\mu}\left(A^+\sinh(k\sqrt{\mu}L) + B^+\cosh(k\sqrt{\mu}L)\right) \\ -A^D_> e^{-kL} &= \sqrt{\mu}\left(A^B\sinh(k\sqrt{\mu}L) + B^B\cosh(k\sqrt{\mu}L)\right) \\ &\Leftrightarrow \\ \tanh\left(k\sqrt{\mu}L\right) &= \frac{-2\sqrt{\mu}}{1+\mu} \qquad \text{(A.5)} \\ A^C_> &= \frac{1}{2}B^+(1-\mu)\sinh\left(k\sqrt{-\mu}L\right)e^{kL} \\ A^D_> &= \frac{1}{2}B^B(1-\mu)\sinh\left(k\sqrt{-\mu}L\right)e^{kL} \end{aligned}$$

$$\Psi(r,\theta,z) = \begin{cases} B^+ J_l(kr)\, e^{\imath l\theta}\left(\sqrt{\mu}\cosh(kz) + \sinh\left(k\sqrt{\mu}z\right)\right) & \text{in A} \\ \begin{cases} B^+\sqrt{\mu}J_l(kr)e^{\imath l\theta}e^{kz} & z < 0 \\ \left(\frac{1}{2}B^+(1-\mu)\sinh\left(k\sqrt{\mu}L\right)e^{kL}\right) J_l(kr)e^{\imath l\theta}e^{-kz} & z > L \end{cases} & \text{in C} \\ \left(B^+\frac{J_l(kr_c)}{J_l(k\sqrt{\mu}r_c)}\right) J_l(mr)e^{\imath l\theta}\left(\sqrt{\mu}\cosh\left(k\sqrt{\mu}z\right) + \sinh\left(k\sqrt{\mu}z\right)\right) & \text{in B} \\ \begin{cases} B^+\sqrt{\mu}J_l(kr)e^{\imath l\theta}e^{kz} & z < 0 \\ \left(\frac{1}{2}B^+(1-\mu)\sinh\left(k\sqrt{\mu}L\right)e^{kL}\right) J_l(kr)e^{\imath l\theta}e^{-kz} & z > L \end{cases} & \text{in D} \end{cases}$$

$$\mu k J_l'(kr_c) + \frac{l\nu}{r_c} J_l(kr_c) = \frac{J_l(kr_c)}{J_l(k\sqrt{\mu}r_c)} J_l'(k\sqrt{\mu}r_c) k\sqrt{\mu}$$

Although a solution appears to exists, it is evident that (A.5) admits no solutions for positive k.

A.4 NORMS OF THE MODES

Given that the solution in the experiment is likely to be a superposition of multiple modes, it is convenient to normalize the solutions so that $\int_V \Psi\Psi^* \mathrm{d}V = 1$ within the cylinder. Restricting the integral to the cylinder is of course mathematically problematic: it is not clear that the integral within the cylinder is sufficient to establish mode orthogonality – nor is it clear that the modes are orthogonal in the first place, except with respect to the azimuthal number l. However, one may hope that the integral outside the cylinder contributes little to the final result and may thus be neglected. One would expect this to be the case for solutions concentrated in the body of the cylinder instead of its boundary, such as the $l = 0$, where the Bessel function achieves its maximum at the center of the cylinder.

For the azimuthal solutions, one needs merely to introduce a factor of $\frac{1}{\sqrt{2\pi}}$. The radial integral does not give a simple result, so only the axial part of the solution can be calculated and simplified.

$$\begin{aligned} Z(z)Z(z) &= \left(\sqrt{-\mu}\cos\left(k\sqrt{-\mu}z\right) + \sin\left(k\sqrt{-\mu}z\right)\right)\left(\sqrt{-\mu}\cos\left(k\sqrt{-\mu}z\right) + \sin\left(k\sqrt{-\mu}z\right)\right) \\ &= -\mu \underbrace{\cos^2\left(k\sqrt{-\mu}z\right)}_{I_1} + \underbrace{\sin^2\left(k\sqrt{-\mu}z\right)}_{I_2} + \sqrt{-\mu}\underbrace{2\cos\left(k\sqrt{-\mu}z\right)\sin\left(k\sqrt{-\mu}z\right)}_{I_3} \end{aligned}$$

$$\begin{aligned} I_1 &= \int_0^L \cos^2(k\sqrt{-\mu}z)\mathrm{d}z \\ &= \frac{L}{2} + \frac{\sin\left(2k\sqrt{-\mu}L\right)}{4k\sqrt{-\mu}} \\ &= \frac{L}{2} + \frac{-4\sqrt{-\mu}\frac{(1+\mu)}{(1-\mu)^2}}{4k\sqrt{-\mu}} \\ &= \frac{L}{2} - \frac{1+\mu}{k\left(1-\mu\right)^2} \end{aligned}$$

$$
\begin{aligned}
I_2 =& \int_0^L \sin^2(k\sqrt{-\mu}z)\mathrm{d}z \\
=& \frac{L}{2} - \frac{\sin\left(2k\sqrt{-\mu}L\right)}{4k\sqrt{-\mu}} \\
=& \frac{L}{2} - \frac{-4\sqrt{-\mu}\frac{(1+\mu)}{(1-\mu)^2}}{4k\sqrt{-\mu}} \\
=& \frac{L}{2} + \frac{1+\mu}{k\left(1-\mu\right)^2}
\end{aligned}
$$

In the above derivations it is convenient to use trigonometric identities and (3.20). Hence we can solve the sine:

$$
\begin{aligned}
\sin\left(2k\sqrt{-\mu}h\right) =& \frac{2\tan\left(k\sqrt{-\mu}h\right)}{1+\tan^2\left(k\sqrt{-\mu}h\right)} \\
=& \frac{2\frac{-2\sqrt{-\mu}}{1+\mu}}{1+\left(\frac{-2\sqrt{-\mu}}{1+\mu}\right)^2} \\
=& -4\sqrt{-\mu}\frac{(1+\mu)}{(1-\mu)^2}
\end{aligned}
$$

$$
\begin{aligned}
I_3 &= \int_0^L 2\cos\left(k\sqrt{-\mu}z\right)\sin\left(k\sqrt{-\mu}z\right)\mathrm{d}z \\
&= \int_0^L \sin\left(2k\sqrt{-\mu}z\right)\mathrm{d}z \\
&= \frac{1-\cos(2k\sqrt{-\mu}L)}{2k\sqrt{-\mu}} \\
&= \frac{1-\left(2\cos^2(k\sqrt{-\mu}L)-1\right)}{2k\sqrt{-\mu}} = \frac{1-\frac{(1+\mu)^2}{(1-\mu)^2}}{k\sqrt{-\mu}} \\
&= \frac{(1-\mu)^2-(1+\mu)^2}{k\sqrt{-\mu}\left(1-\mu\right)^2} = \frac{-4\mu}{k\sqrt{-\mu}\left(1-\mu\right)^2}
\end{aligned}
$$

Similarly to the previous case, the cosine term is solved using the tangent and (3.20):

$$
\begin{aligned}
\cos^2\left(k\sqrt{-\mu}L\right) =& \frac{1}{\tan^2\left(k\sqrt{-\mu}L\right)+1} = \frac{1}{\left(\frac{-2\sqrt{-\mu}}{1+\mu}\right)^2+1} \\
=& \frac{(1+\mu)^2}{(1-\mu)^2}
\end{aligned}
$$

Finally, this gives the normalization factor.

$$\begin{aligned}\int_0^L (Z(z))^2 \,\mathrm{d}z =& -\mu\left(\frac{L}{2} - \frac{1+\mu}{k\,(1-\mu)^2}\right) + \frac{L}{2} + \frac{1+\mu}{k\,(1-\mu)^2} + \sqrt{-\mu}\frac{-4\mu}{k\sqrt{-\mu}\,(1-\mu)^2} \\ =& \frac{L}{2}\,(1-\mu) + \frac{\mu+\mu^2+1+\mu-4\mu}{k\,(1-\mu)^2} \\ =& \frac{L}{2}\,(1-\mu) + \frac{(1-\mu)^2}{k\,(1-\mu)^2} = \frac{L}{2}\,(1-\mu) + \frac{1}{k} \\ =& \frac{kL\,(1-\mu)+2}{2k}\end{aligned}$$

Contribution from outside the cylinder is given by

$$\begin{aligned}\int_{-\infty}^0 e^{kz}\,\mathrm{d}z + \int_L^\infty e^{-kz}\,\mathrm{d}z =& \frac{1}{k} + \frac{e^{-kL}}{k} \\ =& \frac{1+e^{-kL}}{k}\end{aligned}$$

So in total

$$\frac{kL\,(1-\mu)+4+2e^{-kL}}{2k}$$

The normalized Ψ-functions are thus

$$\begin{aligned}\Psi_{l,n,m} = &\left(\int_0^{r_c} u J_l^2(ku)\mathrm{d}u\right)^{-\frac{1}{2}} \sqrt{\frac{2k}{kL\,(1-\mu)+2+4+2e^{-kL}}} \\ &\times J_l\,(kr)\,\frac{e^{\imath l\theta}}{\sqrt{2\pi}}\left(\sqrt{-\mu}\cos\left(k\sqrt{-\mu}z\right) + \sin\left(k\sqrt{-\mu}z\right)\right) \quad \text{(A.6)}\end{aligned}$$

B

EXCITATION OF MAGNETOSTATIC MODES

B.1 ENERGETICS OF MAXWELL'S EQUATIONS

The rate at which energy enters or leaves volume V bounded by surface S can be expressed as a surface integral of the energy current $\vec{P}$. In order to satisfy the conservation of energy, the energy entering the volume must equal to the energy stored in the volume (w) and the power dissipated in the volume P_d:

$$-\int_S \vec{P}\cdot \mathrm{d}\vec{S} = -\int_V \nabla\cdot\vec{P}\mathrm{d}V = \int_V \dot{w}\mathrm{d}V + \int_V P_d \mathrm{d}V.$$

As this expression should be valid for any volume, we can take the limit of infinitesimal volume and obtain the following differential equation:

$$\nabla\cdot\vec{P} + \dot{w} + P_d = 0.$$

In electrodynamics, this is expressed with the Poynting theorem:

$$\nabla\cdot\left(\vec{E}\times\vec{H}\right) + \vec{H}\cdot\dot{\vec{B}} + \vec{E}\cdot\dot{\vec{D}} + \vec{E}\cdot\vec{J} = 0. \tag{B.1}$$

The quantity $\vec{E}\times\vec{H}$ is known as the Poynting vector, and it corresponds to the electromagnetic energy current $\vec{P}$. For sinusoidally varying complex fields ($E(t) = Ee^{i\omega t}$) , the Poynting theorem takes the following form [34, p. 117]:

$$\nabla\cdot\left(\vec{E}\times\vec{H}^*\right) + i\omega\left(\vec{H}^*\cdot\vec{B} - \vec{E}\cdot\vec{D}^*\right) + \vec{E}\cdot\vec{J}^* = 0 \tag{B.2}$$

Time average over the period $T = \frac{2\pi}{\omega}$ is then easily obtained by taking the real part [34, p. 116]. Hence, the average of the divergence of power is

$$\left\langle \nabla\cdot\vec{P}\right\rangle = \left\langle \nabla\cdot\left(\vec{E}\times\vec{H}^*\right)\right\rangle = \frac{1}{2}\,\mathrm{Re}\left\{\nabla\cdot\left(\vec{E}\times\vec{H}^*\right)\right\}.$$

For magnetostatic modes, the equation naturally applies to the first-order quantities such $\vec{e}$ and $\vec{h}$. Applying vector identities and $\nabla\times\vec{h} = 0$ allows the simplification of the expression:

$$\begin{aligned}\nabla \cdot \left(\vec{e} \times \vec{h^*}\right) =& \vec{h^*} \cdot (\nabla \times \vec{e}) - \vec{e} \cdot \left(\nabla \times \vec{h^*}\right) \\ =& \vec{h^*} \cdot (\nabla \times \vec{e}) \,.\end{aligned}$$

Using Faraday's law (3.4) and introducing Ψ allows further simplification:

$$\begin{aligned}\vec{h^*} \cdot (\nabla \times \vec{e}) =& -i\omega \vec{h^*} \cdot \vec{b} \\ =& -i\omega \left(\nabla \Psi^*\right) \cdot \vec{b} \\ =& -i\omega \left[\nabla \cdot \left(\Psi^* \vec{b}\right) - \Psi^* \nabla \cdot \vec{b}\right] \\ =& -i\omega \nabla \cdot \left(\Psi^* \vec{b}\right) \\ =& \nabla \cdot \vec{P}.\end{aligned}$$

The last equality implies that $\vec{P} = -i\omega\Psi^*\vec{b} + \vec{u}$ with $\nabla \cdot \vec{u} = 0$. It fulfills the Poynting equation (B.2) and gives the correct results for measurable quantities. The vector $\vec{u}$ is then more like a gauge transformation which may be arbitrarily chosen [34, p. 170]. With this the expression for the time-averaged power becomes

$$\left\langle \vec{P} \right\rangle = \frac{1}{2} \operatorname{Re}\left\{-i\omega\Psi^*\vec{b}\right\}. \tag{B.3}$$

B.2 POYNTING VECTOR FOR MAGNETOSTATIC MODES IN A CYLINDER

The Poynting vector has r, θ, and z components. The calculations are straightforward using the definition of $\vec{b}$ and (3.9).

$$\begin{aligned}\left\langle \vec{P} \right\rangle \cdot \vec{e_r} =& -\frac{1}{2} \operatorname{Re}\{i\omega\Psi^*\vec{b}\} \cdot \vec{e_r} \\ =& -\frac{1}{2} \operatorname{Re}\{i\omega\Psi^* b_r\} \\ =& -\frac{1}{2} \operatorname{Re}\{i\omega\Psi^* \left(h_r + 4\pi m_r\right)\} \\ =& -\frac{1}{2} \operatorname{Re}\{i\omega\Psi^* \left(\partial_r\Psi + \kappa\partial_r\Psi - \frac{i\nu}{r}\partial_\theta\Psi\right)\} \\ =& -\frac{1}{2} \operatorname{Re}\{\omega \left(i\Psi^*\partial_r\Psi + i\kappa\Psi^*\partial_r\Psi + \frac{il\nu}{r}|\Psi|^2\right)\} \\ =& 0.\end{aligned}$$

For the azimuthal component the magnetization is given by (3.10):

$$\begin{aligned}
\left\langle \vec{P} \right\rangle \cdot \vec{e_\theta} =& -\frac{1}{2}\,\mathrm{Re}\{i\omega\Psi^*\vec{b}\}\cdot\vec{e_\theta}\\
=& \frac{-1}{2}\,\mathrm{Re}\{i\omega\Psi^* b_\theta\}\\
=& -\frac{1}{2}\,\mathrm{Re}\{i\omega\Psi^*\left(h_\theta + 4\pi m_\theta\right)\}\\
=& -\frac{1}{2}\,\mathrm{Re}\{i\omega\Psi^*\left(\frac{1}{r}\partial_\theta\Psi + i\nu\partial_r\Psi + \frac{\kappa}{r}\partial_\theta\Psi\right)\}\\
=& -\frac{1}{2}\,\mathrm{Re}\{i\omega\Psi^*\left(\frac{il\Psi}{r} + i\nu\partial_r\Psi + \frac{il\kappa}{r}\Psi\right)\}\\
=& \frac{1}{2}\,\mathrm{Re}\{\omega\left(\frac{l|\Psi|^2}{r} + \nu\Psi^*\partial_r\Psi + \frac{l\kappa}{r}|\Psi|^2\right)\}\\
=& \frac{\omega}{2}\left(\frac{l|\Psi|^2}{r}\left[1+\kappa\right] + \nu\Psi^*\partial_r\Psi\right)\\
=& \frac{\omega}{2}\left(\frac{l|\Psi|^2}{r}\mu + \nu\Psi^*\partial_r\Psi\right).
\end{aligned}$$

Finally, to first order we neglect the magnetization in the axial direction:

$$\begin{aligned}
\left\langle \vec{P} \right\rangle \cdot \vec{e_z} =& -\frac{1}{2}\,\mathrm{Re}\{i\omega\Psi^*\vec{b}\}\cdot\vec{e_z}\\
=& -\frac{1}{2}\,\mathrm{Re}\{i\omega\Psi^* b_z\}\\
=& -\frac{1}{2}\,\mathrm{Re}\{i\omega\Psi^* h_z\}\\
=& -\frac{1}{2}\,\mathrm{Re}\{i\overbrace{\omega\Psi^*\partial_z\Psi}^{\text{real}}\}\\
=& 0.
\end{aligned}$$

Hence, the final results for the pointing vector only contains the azimuthal component:

$$\left\langle \vec{P} \right\rangle = \left(0, \frac{\omega}{2}\left(\frac{l|\Psi|^2}{r}\mu + \nu\Psi^*\partial_r\Psi\right), 0\right). \tag{B.4}$$

In the simplest radial case where $l = 0$, the expression further simplifies to

$$\langle P_\theta \rangle = \frac{\omega}{2}\nu\Psi^*\partial_r\Psi. \tag{B.5}$$

B.3 POWER ABSORPTION OF THE $l = 0$ MODE

The modes are excited with an rf field leaking through a roughly circular aperture. The exact form of the field is complex and not very

well known, however the field is expected to decay exponentially along the z-axis with penetration length of $\lambda \approx 0.008$cm. The radial profile of the field may be approximated in various ways. Simulations with Gaussian, linear, and second degree decay along the radial direction produce very similar results, so it seems the shape of the decaying potential in the radial direction is not very crucial. The following profile is chosen to model the exciting field:

$$g(r,\theta,z) = f(r)\frac{e^{-\frac{z}{\lambda}}}{\sqrt{2\pi}},$$

with $f(r)$ the form of the radial field, assumed to be either Gaussian, linearly decreasing to the edges, or a second-degree polynomial. Given that the Poynting vector only has an azimuthal component, the energy flow is perpendicular to a plane stretching from the center of the cylinder to its edge. Hence the power flow through that surface per unit area is given by

$$P = \frac{\int_S \langle P_\theta \rangle \, \mathrm{d}S}{S} = \frac{\int_0^L \int_0^{r_c} \langle P_\theta \rangle \, r\mathrm{d}r\mathrm{d}z}{Lr_c}. \tag{B.6}$$

The Ψ in (B.5) is unlikely to contain only one mode, so assuming orthogonality of the modes (as discussed in A.4), Ψ can be decomposed into a linear combination of the solutions $\Psi_{0,n,m}$ with coefficients given by

$$c_{0,n,m} = \frac{1}{\sqrt{\int_V g^2(r,\theta,z) r\mathrm{d}r\mathrm{d}\theta\mathrm{d}z}} \int_V \Psi_{0,n,m}(r,\theta,z) g^*(r,\theta,z) r\mathrm{d}r\mathrm{d}\theta\mathrm{d}z. \tag{B.7}$$

(The prefactor is the normalization factor for g and V is the volume of the cylinder.) Once again the radial integral must be calculated numerically while the axial integral is more amenable to explicit integration:

$$\begin{aligned}
&\int_0^L \left(e^{-\frac{z}{\lambda}}\right)\left(\sqrt{-\mu}\cos\left(k\sqrt{-\mu}z\right) + \sin\left(k\sqrt{-\mu}z\right)\right)\mathrm{d}z \\
&= \sqrt{-\mu}\underbrace{\int_0^L e^{-\frac{z}{\lambda}}\cos\left(k\sqrt{-\mu}z\right)\mathrm{d}z}_{I_1} + \underbrace{\int_0^h e^{-\frac{z}{\lambda}}\sin\left(k\sqrt{-\mu}z\right)\mathrm{d}z}_{I_2} \\
&= \sqrt{-\mu}I_1 + I_2.
\end{aligned}$$

The integral is most comfortably evaluateds using Euler's formula $e^{i\theta} = \cos\theta + i\sin\theta$ and taking real and imaginary parts at the end of the calculation:

$$
\begin{aligned}
I_1 + iI_2 &= \int_0^L e^{\left(-\frac{1}{\lambda} + ik\sqrt{-\mu}\right)z} \mathrm{d}z \\
&= \int_0^L e^{cz} \mathrm{d}z \\
&= \frac{1}{c}\left(e^{cL} - 1\right) \\
&= \frac{c^*\left(e^{-\frac{L}{\lambda}}\cos(k\sqrt{-\mu}L) + ie^{-\frac{L}{\lambda}}\sin(k\sqrt{-\mu}L) - 1\right)}{|c|^2}.
\end{aligned}
$$

The constant c, its complement, and the square of the modulus are given by

$$
\begin{aligned}
c &= \frac{i\lambda k\sqrt{-\mu} - 1}{\lambda} \\
c^* &= -\frac{i\lambda k\sqrt{-\mu} + 1}{\lambda} \\
|c|^2 &= \frac{1 - k^2\lambda^2\mu}{\lambda^2}.
\end{aligned}
$$

Substituting these gives the result of the integral:

$$
\begin{aligned}
I_1 + iI_2 &= -\frac{\lambda^2}{1 - k^2\lambda^2\mu}\frac{i\lambda k\sqrt{-\mu} + 1}{\lambda}\left(e^{-\frac{L}{\lambda}}\left[\cos\left(k\sqrt{-\mu}L\right) + i\sin\left(k\sqrt{-\mu}L\right)\right] - 1\right) \\
&= \frac{\lambda}{1 - k^2\lambda^2\mu}\left[\left(1 - e^{-\frac{L}{\lambda}}\left[\cos\left(k\sqrt{-\mu}h\right) - \lambda k\sqrt{-\mu}\sin\left(k\sqrt{-\mu}h\right)\right]\right)\right. \\
&\quad \left. + i\left(\lambda k\sqrt{-\mu} - e^{-\frac{L}{\lambda}}\left[\lambda k\sqrt{-\mu}\cos\left(k\sqrt{-\mu}h\right) + \sin\left(k\sqrt{-\mu}h\right)\right]\right)\right] \\
I_1 &= \lambda\frac{1 - e^{-\frac{L}{\lambda}}\left(\cos(k\sqrt{-\mu}L) - \lambda k\sqrt{-\mu}\sin(k\sqrt{-\mu}L)\right)}{1 - k^2\lambda^2\mu} \\
I_2 &= \lambda\frac{\lambda k\sqrt{-\mu} - e^{-\frac{L}{\lambda}}\left(\lambda k\sqrt{-\mu}\cos(k\sqrt{-\mu}L) + \sin(k\sqrt{-\mu}L)\right)}{1 - k^2\lambda^2\mu}.
\end{aligned}
$$

The expression for the axial integral is then

$$
\begin{aligned}
\sqrt{-\mu}I_1 + I_2 &= \frac{\lambda}{1 - k^2\lambda^2\mu}\left(\sqrt{-\mu}\left[1 - e^{-\frac{L}{\lambda}}\left(\cos\left(k\sqrt{-\mu}L\right) - \lambda k\sqrt{-\mu}\sin\left(k\sqrt{-\mu}L\right)\right)\right]\right. \\
&+ \left.\lambda k\sqrt{-\mu} - e^{-\frac{L}{\lambda}}\left(\lambda k\sqrt{-\mu}\cos\left(k\sqrt{-\mu}L\right) + \sin\left(k\sqrt{-\mu}L\right)\right)\right) \\
&= \frac{\lambda}{1 - k^2\lambda^2\mu}\left[\sqrt{-\mu}(1 + \lambda k)\left(1 - e^{-\frac{L}{\lambda}}\cos\left(k\sqrt{-\mu}L\right)\right)\right. \qquad \text{(B.8)} \\
&- \left.(\lambda k\mu + 1)e^{-\frac{L}{\lambda}}\sin\left(k\sqrt{-\mu}L\right)\right]. \qquad \text{(B.9)}
\end{aligned}
$$

The integral over θ removes all the factors of $\frac{1}{\sqrt{2\pi}}$ and leaves just the integral over r. From (A.6), (B.7), and(B.8) the expression for $c_{0,n,m}$ becomes

$$c_{0,n,m} = \sqrt{\frac{2k}{kL(1-\mu)+2}} \frac{\lambda(\mu-1)}{1-k^2\lambda^2\mu} \frac{k\int_0^{r_c} rJ_l(kr) f^*(r)\mathrm{d}r}{\sqrt{\int_0^{\frac{r_c}{k}} uJ_l^2(u)\mathrm{d}u}} \times \left[\frac{\sqrt{-\mu}(1-\lambda k)}{\mu-1}\left(1-e^{-\frac{L}{\lambda}}\cos\left(k\sqrt{-\mu}L\right)\right) + e^{-\frac{L}{\lambda}}\sin\left(k\sqrt{-\mu}L\right)\right].$$

With this, we may express $\Psi = \sum_{n,m} c_{0,n,m}\Psi_{0,n,m}$. From (B.5) and (B.6), the power per unit area becomes

$$\begin{aligned} P =& \frac{\int_0^L \int_0^{r_c} \frac{\omega}{2}\nu\Psi^*\partial_r\Psi r\mathrm{d}r\mathrm{d}z}{Lr_c} \\ =& \frac{\omega\nu}{2Lr_c}\sum_{n,m}\sum_{p,q} c^*_{0,n,m}c_{0,p,q}\int_0^L\int_0^{r_c}\Psi^*_{0,n,m}\partial_r\Psi_{0,p,q}r\mathrm{d}r\mathrm{d}z \\ =& \frac{\omega\nu}{2Lr_c}\sum_{n,m}\sum_{p,q} c_{0,n,m}c_{0,p,q}\int_0^L\int_0^{r_c}\Psi_{0,n,m}\partial_r\Psi_{0,p,q}r\mathrm{d}r\mathrm{d}z. \end{aligned}$$

To a first approximation, we neglect the cross terms $c_{0,n,m}c_{0,p,q}$ where $n \neq p, m \neq q$, and the resulting expression is

$$\begin{aligned} P &= \frac{\omega\nu(\omega)}{2Lr_c}\sum_{n,m} c_{0,n,m}c_{0,n,m}\int_0^L\int_0^{r_c}\Psi_{0,n,m}\partial_r\Psi_{0,n,m}r\mathrm{d}r\mathrm{d}z \\ &= \frac{\omega\nu(\omega)}{2Lr_c}\sum_{n,m}\frac{2k}{kL(1-\mu_{n,m})+2}\int_0^L Z^2(z)\mathrm{d}z \\ &\times \left[\frac{\lambda(\mu_{n,m}-1)}{1-k^2\lambda^2\mu_{n,m}}\right]^2 \frac{\left(k_{n,m}\int_0^{r_c} rJ_l(kr)f^*(r)\mathrm{d}r\right)^2}{\int_0^{k_{n,m}r_c} uJ_l^2(u)\mathrm{d}u} \\ &\times \left[\frac{\sqrt{-\mu_{n,m}}(1-\lambda k_{n,m})}{\mu_{n,m}-1}\left(1-e^{-\frac{L}{\lambda}}\cos\left(k_{n,m}\sqrt{-\mu}L\right)\right)\right. \\ &+ \left. e^{-\frac{L}{\lambda}}\sin\left(k_{n,m}\sqrt{-\mu}L\right)\right]^2 \times \frac{\int_0^{k_{n,m}r_c} uJ_0(r)J_0'(r)\mathrm{d}u}{2\pi\int_0^{k_{n,m}r_c} uJ_l^2(ku)\mathrm{d}u}. \end{aligned}$$

C

A GALLERY OF MODES

C.1 MAGNETIC POTENTIAL

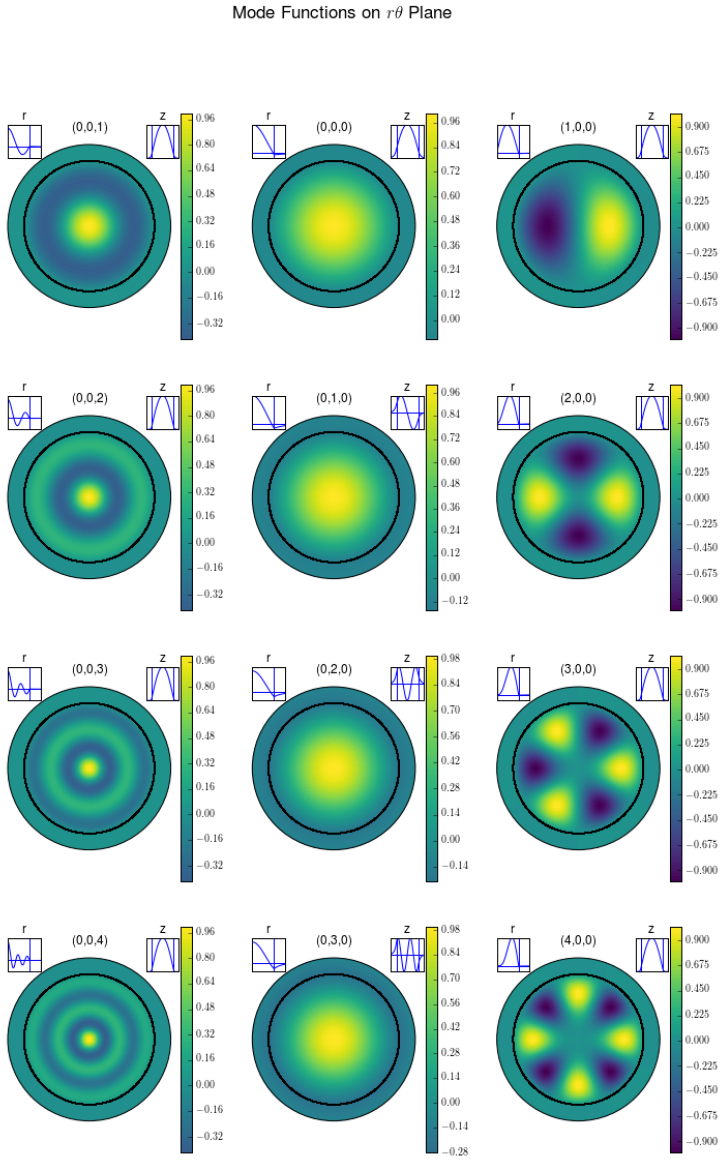

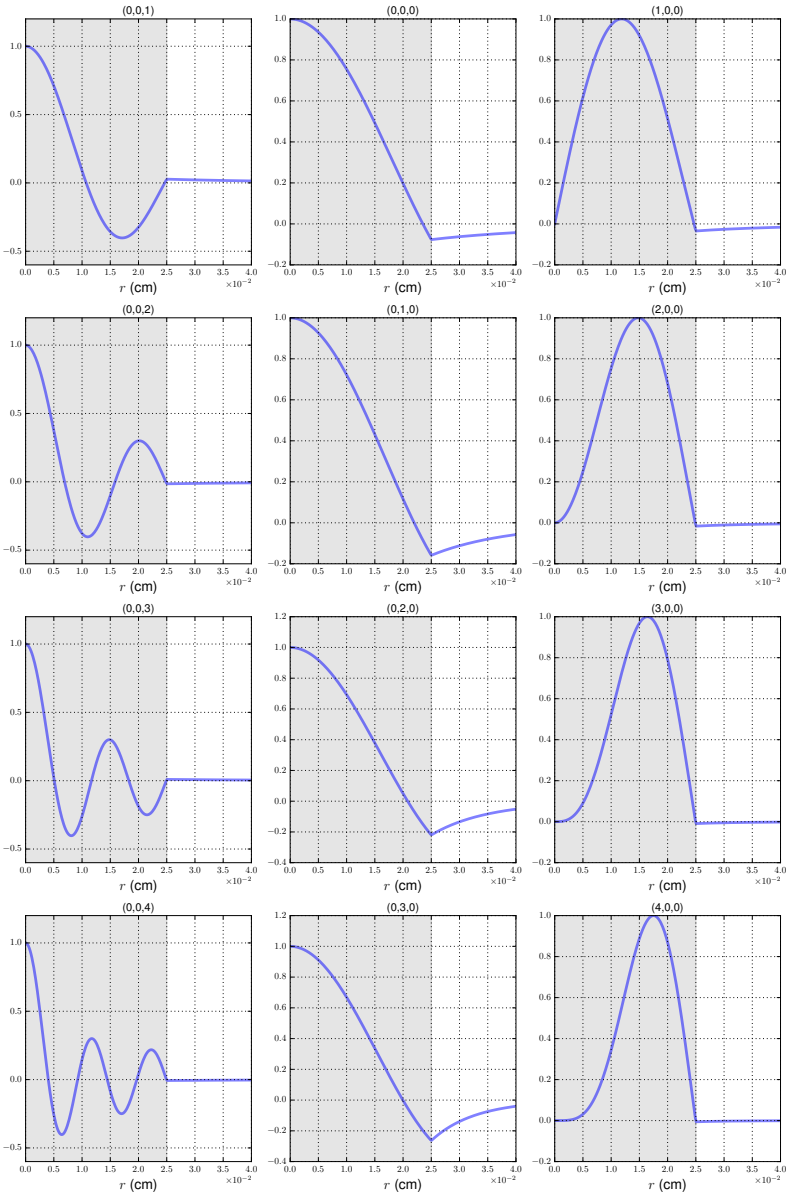

Figure C.1:

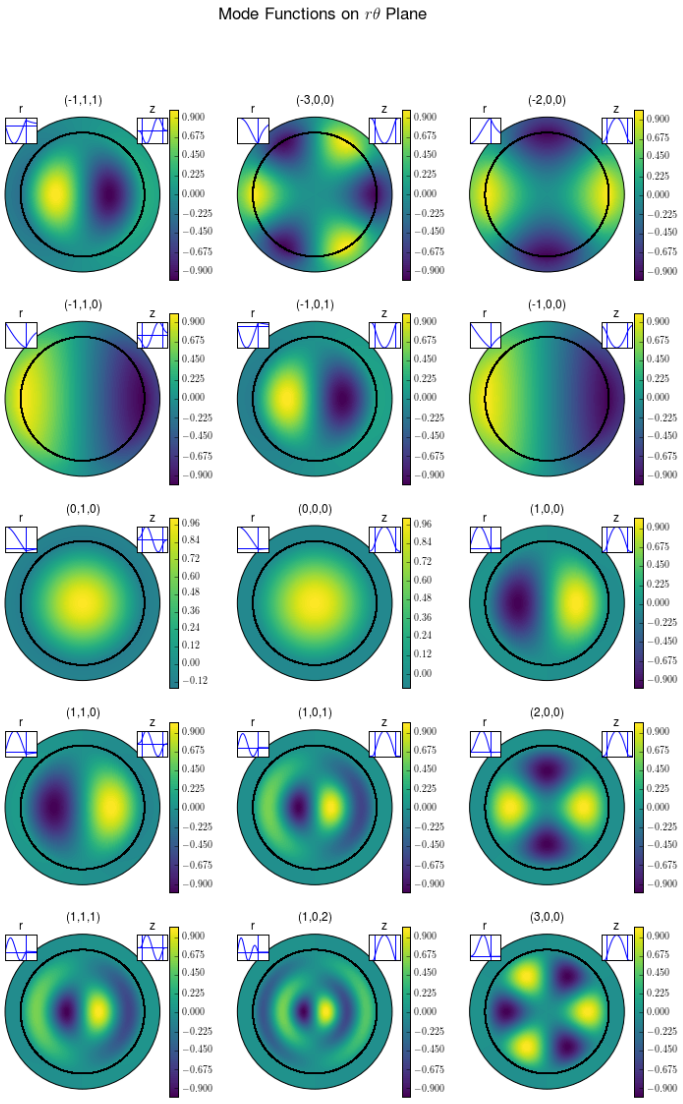
Mode Functions on $r\theta$ Plane
(-1,1,1)
(-3,0,0)
(-2,0,0)
(-1,1,0)
(-1,0,1)
(-1,0,0)
(0,1,0)
(0,0,0)
(1,0,0)
(1,1,0)
(1,0,1)
(2,0,0)
(1,1,1)
(1,0,2)
(3,0,0)
r
z

Figure C.2:

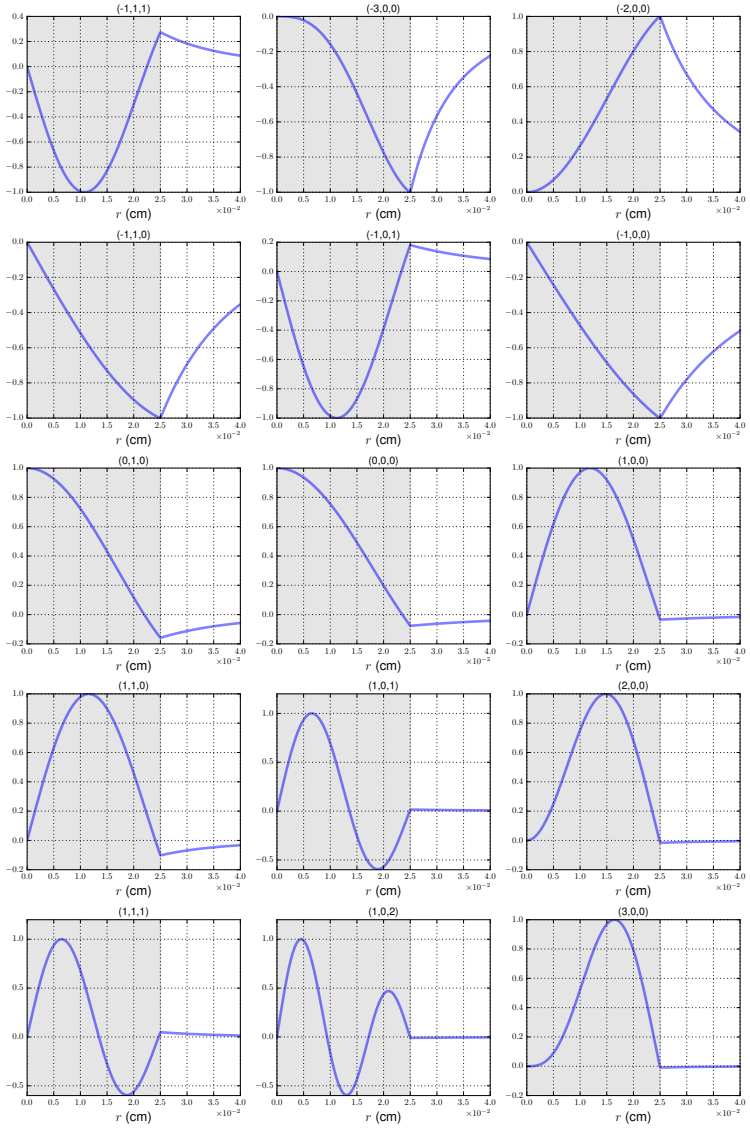
(-1,1,1)
(-3,0,0)
(-2,0,0)
(-1,1,0)
(-1,0,1)
(-1,0,0)
(0,1,0)
(0,0,0)
(1,0,0)
(1,1,0)
(1,0,1)
(2,0,0)
(1,1,1)
(1,0,2)
(3,0,0)
r (cm)
×10⁻²

Figure C.3:

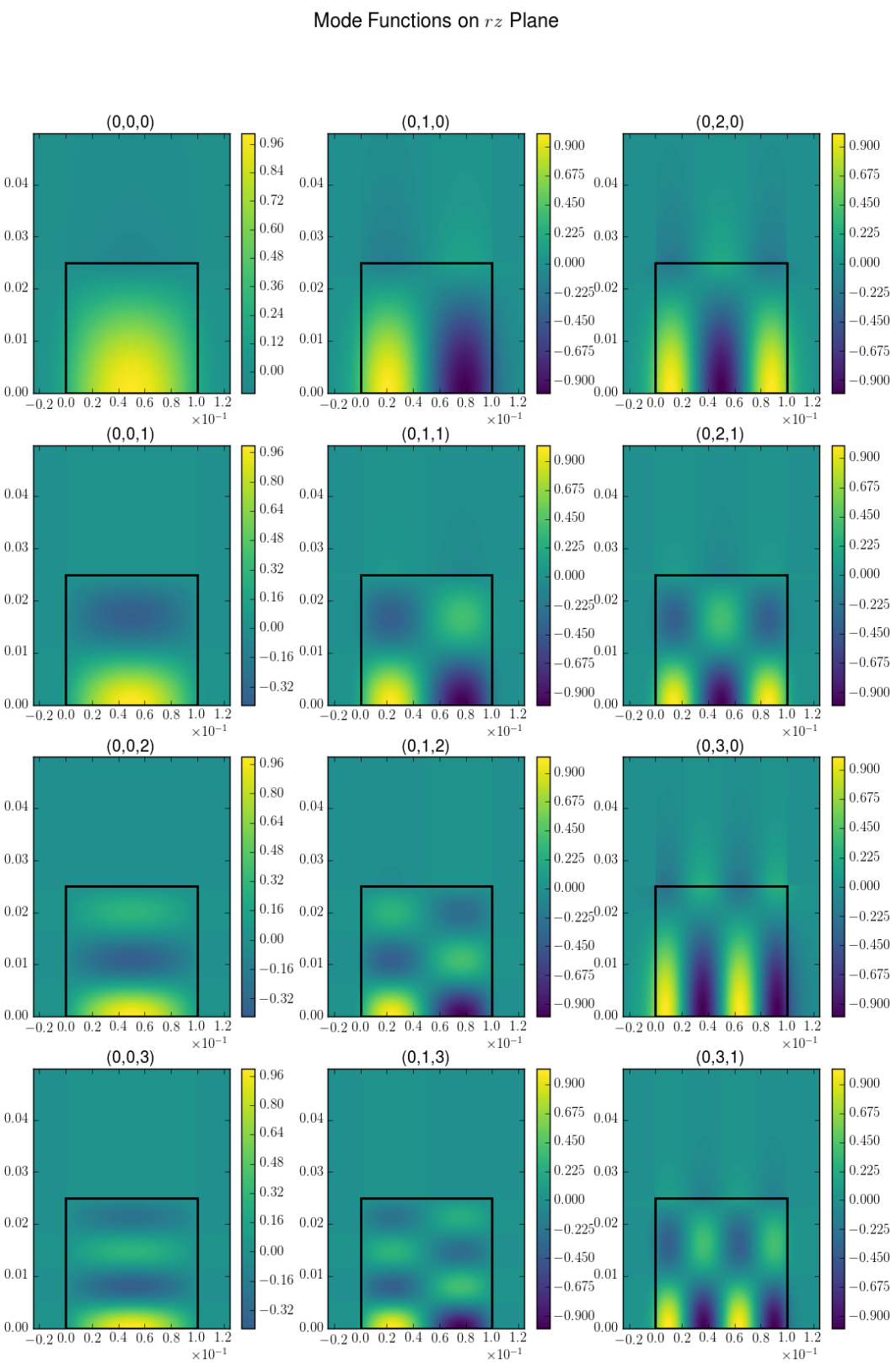
Mode Functions on rz Plane
(0,0,0)
(0,1,0)
(0,2,0)
(0,0,1)
(0,1,1)
(0,2,1)
(0,0,2)
(0,1,2)
(0,3,0)
(0,0,3)
(0,1,3)
(0,3,1)

Figure C.4:

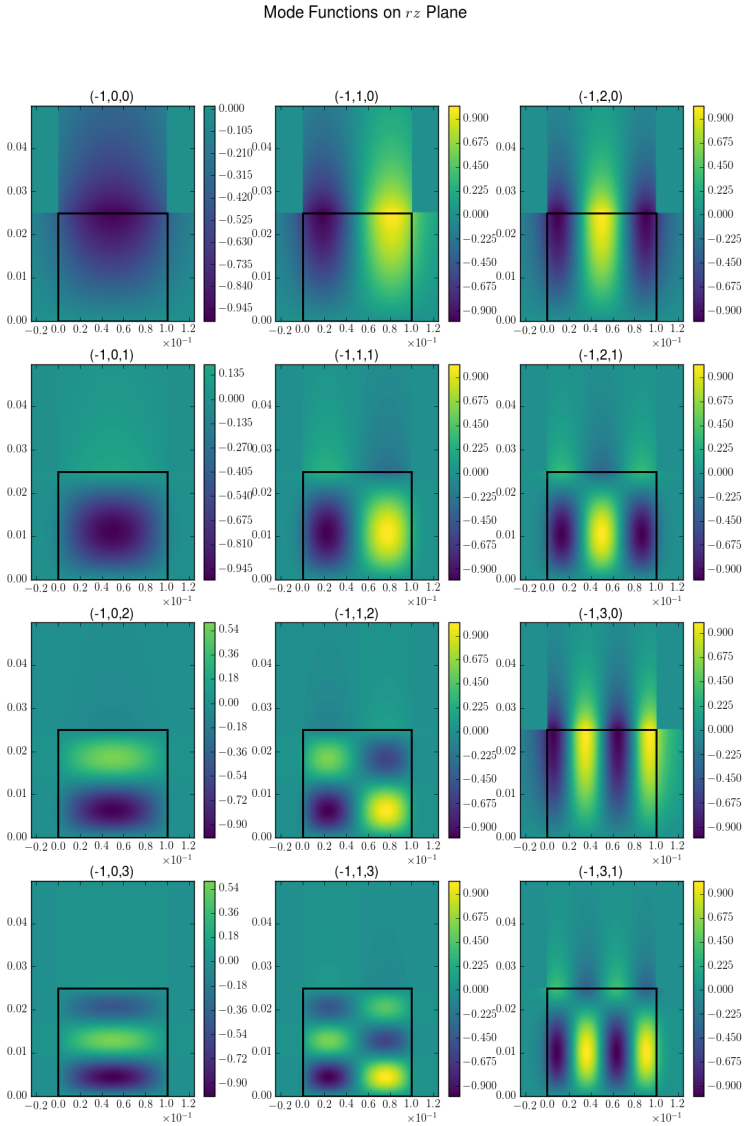
Mode Functions on rz Plane
(-1,0,0)
(-1,1,0)
(-1,2,0)
(-1,0,1)
(-1,1,1)
(-1,2,1)
(-1,0,2)
(-1,1,2)
(-1,3,0)
(-1,0,3)
(-1,1,3)
(-1,3,1)

Figure C.5:

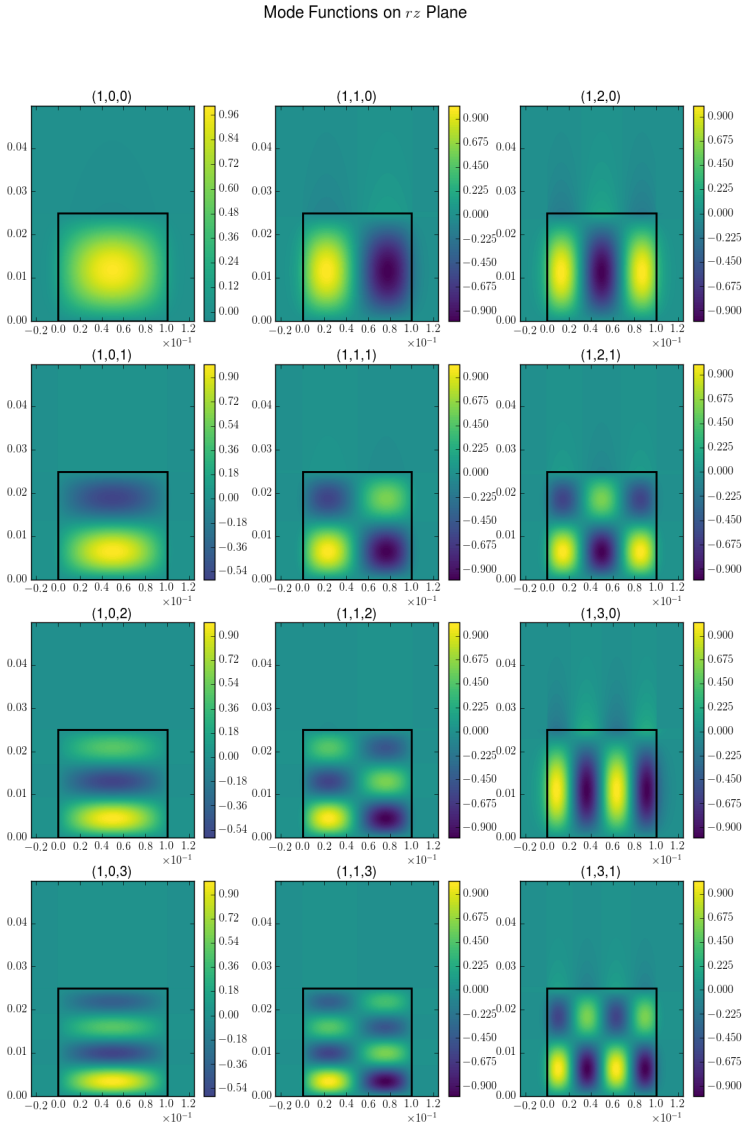
Mode Functions on rz Plane
(1,0,0)
(1,1,0)
(1,2,0)
(1,0,1)
(1,1,1)
(1,2,1)
(1,0,2)
(1,1,2)
(1,3,0)
(1,0,3)
(1,1,3)
(1,3,1)

Figure C.6:

C.2 FIELDS

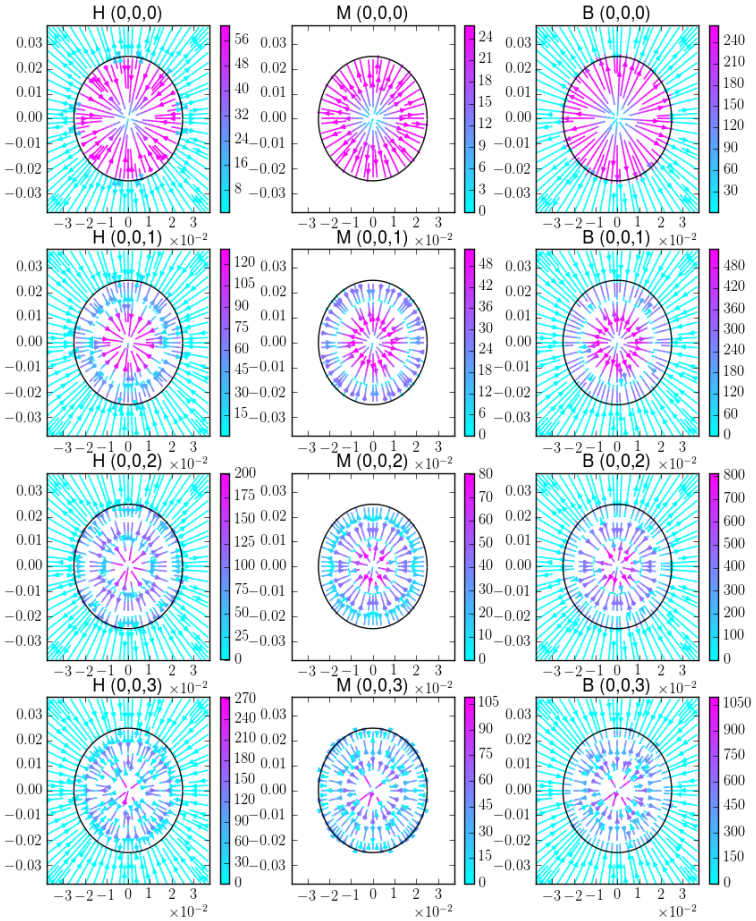
H (0,0,0)
M (0,0,0)
B (0,0,0)
H (0,0,1) ×10⁻²
M (0,0,1) ×10⁻²
B (0,0,1) ×10⁻²
H (0,0,2) ×10⁻²
M (0,0,2) ×10⁻²
B (0,0,2) ×10⁻²
H (0,0,3) ×10⁻²
M (0,0,3) ×10⁻²
B (0,0,3) ×10⁻²
×10⁻²

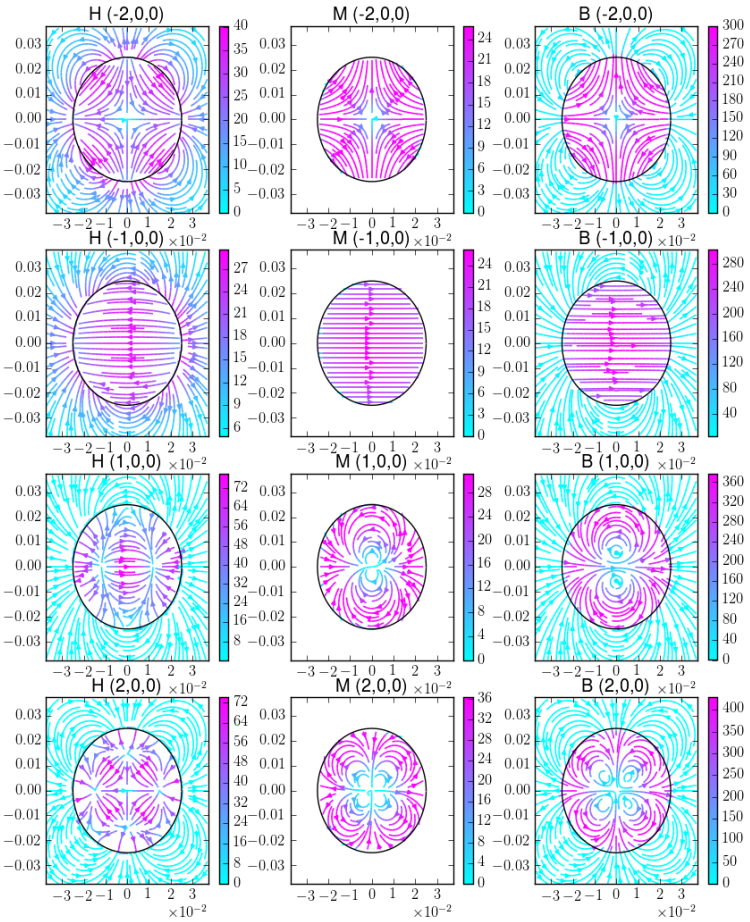
H (-2,0,0)
M (-2,0,0)
B (-2,0,0)
H (-1,0,0) ×10⁻²
M (-1,0,0) ×10⁻²
B (-1,0,0) ×10⁻²
H (1,0,0) ×10⁻²
M (1,0,0) ×10⁻²
B (1,0,0) ×10⁻²
H (2,0,0) ×10⁻²
M (2,0,0) ×10⁻²
B (2,0,0) ×10⁻²
×10⁻²

Figure C.7:

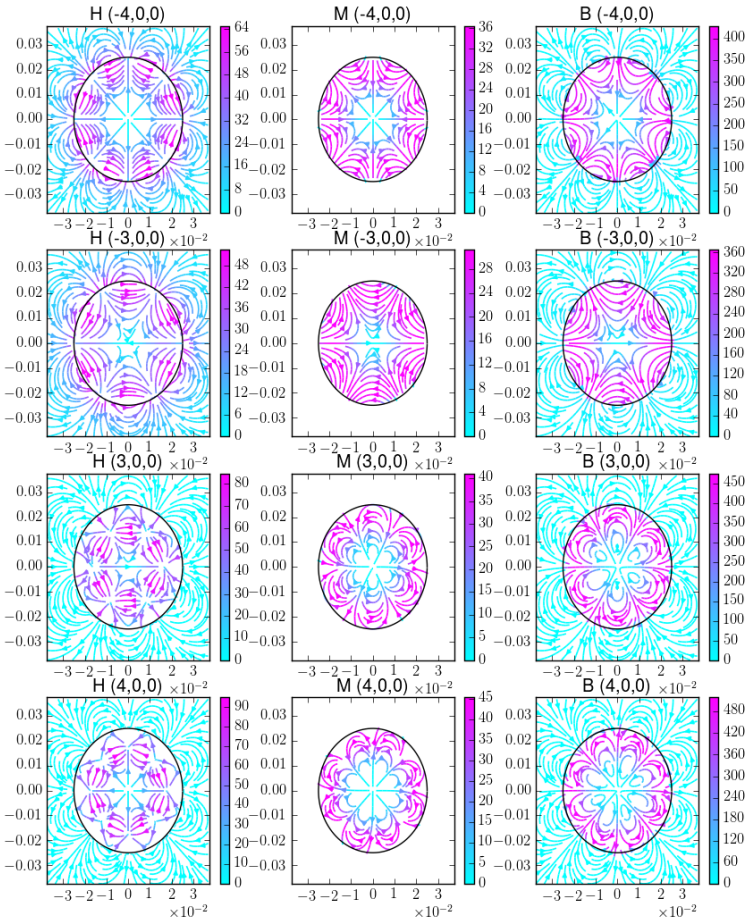
H (-4,0,0)
M (-4,0,0)
B (-4,0,0)
H (-3,0,0)
M (-3,0,0)
B (-3,0,0)
H (3,0,0)
M (3,0,0)
B (3,0,0)
H (4,0,0)
M (4,0,0)
B (4,0,0)
×10⁻²

Figure C.8:

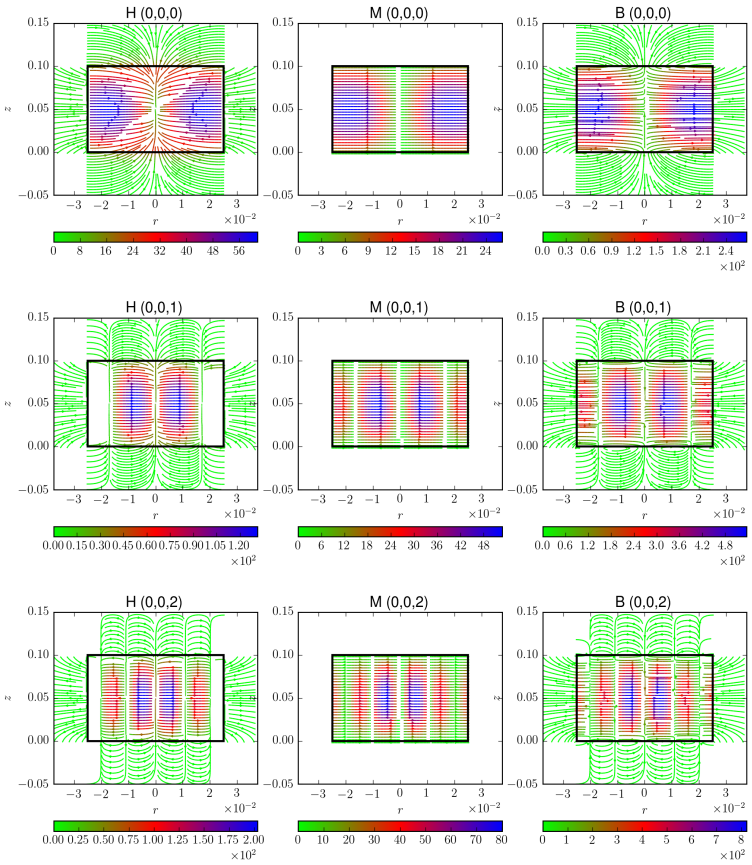

Figure C.9:

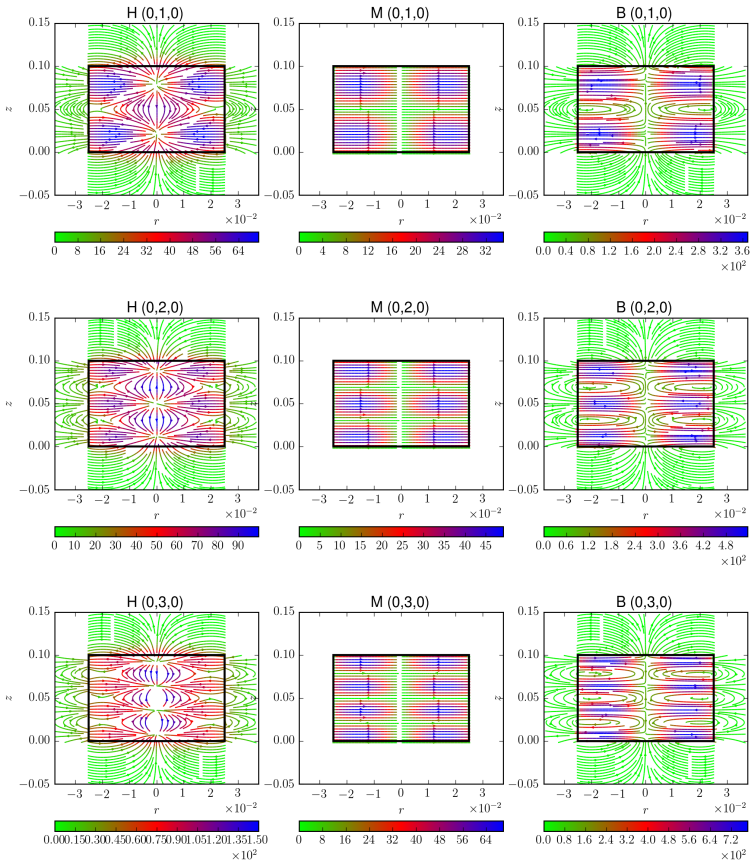

Figure C.10:

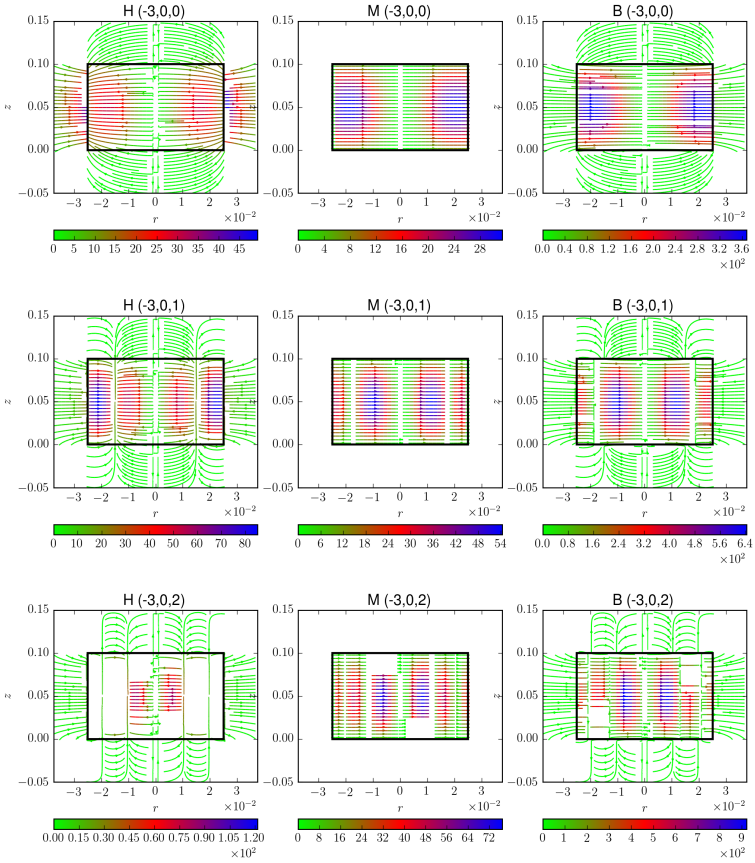

Figure C.11:

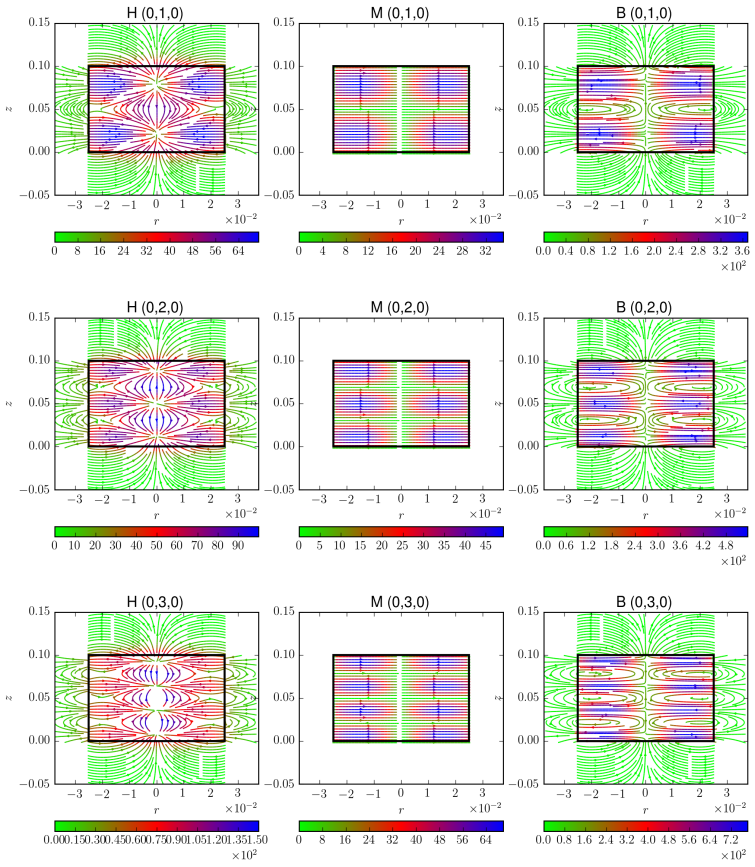

Figure C.12:

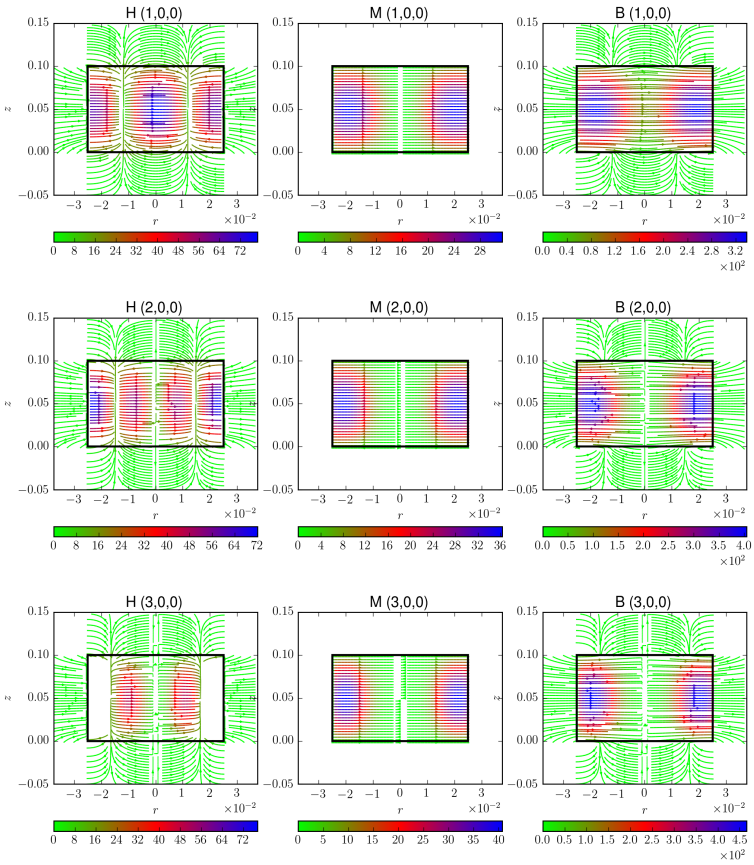

Figure C.13:

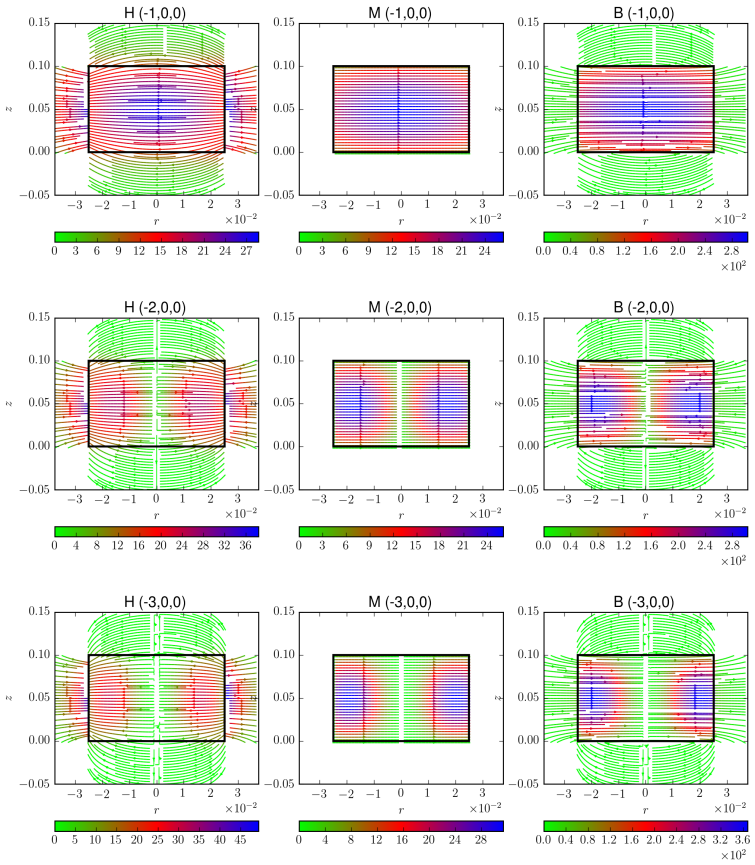

Figure C.14:

C.3 RADIAL MAGNETIC FIELD $\vec{b}_r(r)$

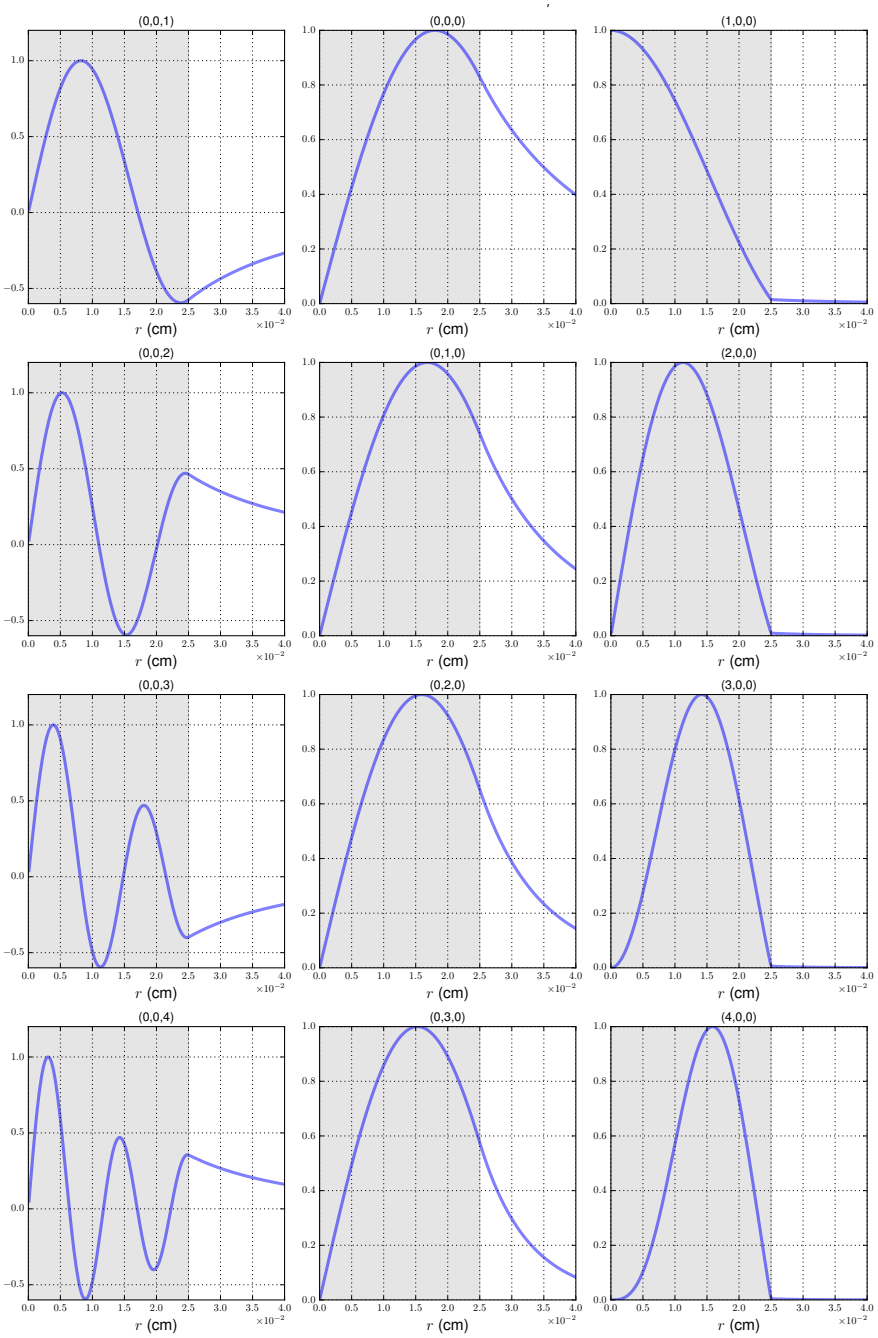

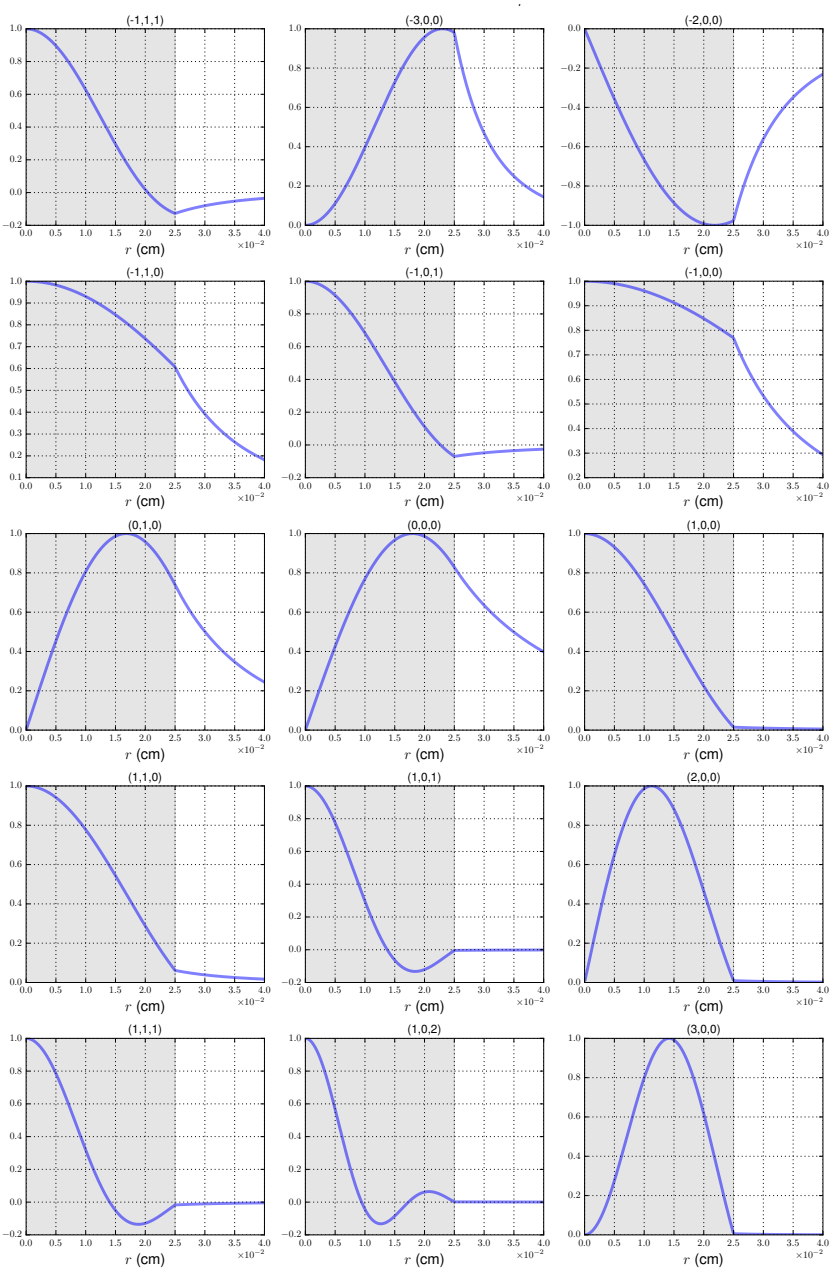
(-1,1,1)
(-3,0,0)
(-2,0,0)
(-1,1,0)
(-1,0,1)
(-1,0,0)
(0,1,0)
(0,0,0)
(1,0,0)
(1,1,0)
(1,0,1)
(2,0,0)
(1,1,1)
(1,0,2)
(3,0,0)
r (cm)
×10⁻²

BIBLIOGRAPHY

[1] A. Aharoni. *Introduction to the Theory of Ferromagnetism*. International Series of Monographs on Physics. Clarendon Press, 2000 (cit. on p. 5).

[2] Y. Aharonov and D. Bohm. "Significance of Electromagnetic Potentials in the Quantum Theory." In: *Phys. Rev.* 115 (3 Aug. 1959), pp. 485–491. DOI: 10.1103/PhysRev.115.485 (cit. on p. 4).

[3] Rodrigo E. Arias. "Magnetostatic Modes in Samples With Inhomogeneous Internal Fields." In: *IEEE Magnetics Letters* 6 (2015) (cit. on p. 35).

[4] Marco Beleggia, Marc De Graef, Yonko T. Millev, David A. Goode, and George Rowlands. "Demagnetization Factors for Elliptic Cylinders." In: *Journal of Physics D: Applied Physics* 38.18 (2005), p. 3333 (cit. on p. 18).

[5] Felix Bloch. "Zur Theorie des Ferromagnetismus." In: *Zeitschrift für Physik* 61.3-4 (Mar. 1930), pp. 206–219. DOI: 10.1007/BF01339661 (cit. on p. 5).

[6] S. Bornmann, A. Schönecker, and W. Haubenreisser. "Magnetostatic mode pattern and mode spectrum analysis in finite ferromagnetic circular disks." In: *physica status solidi ...* 11 (1972), p. 207. DOI: 10.1002/pssa.2210110123 (cit. on pp. 12, 32).

[7] William Fuller Brown, Jr. "Single-Domain Particles : New Uses of Old Theorems." In: *American Journal of Physics* 28.6 (1960), pp. 542–551. DOI: 10.1119/1.1935878 (cit. on p. 18).

[8] John B. Carlson. "Lodestone Compass: Chinese or Olmec Primacy?" In: *Science* 189.4205 (1975), pp. 753–760. DOI: 10.1126/science.189.4205.753 (cit. on p. 3).

[9] Du-Xing Chen, J.A. Brug, and Ronald B. Goldfarb. "Demagnetizing factors for cylinders." In: *IEEE Transactions on Magnetics* 27.4 (1991), pp. 3601–3619. DOI: 10.1109/20.102932 (cit. on p. 18).

[10] L. R. Corruccini, D. M. Osheroff D. D .and Lee, and R. C. Richardson. "Spin-Wave Phenomena in Liquid ^{3}He Systems *." In: 8.1698 (1972), pp. 229–254 (cit. on p. 12).

[11] R. W. Damon and J. R. Eshbach. "Magnetostatic modes of a ferromagnet slab." In: *Journal of Physics and Chemistry of Solids* 19.3 (May 1961), pp. 308–320. DOI: 10.1016/0022-3697(61)90041-5 (cit. on p. 12).

[12] R. W. Damon and H. Van De Vaart. "Dispersion of long-wavelength spin waves from pulse-echo experiments." In: *Physical Review Letters* 12.21 (1964), pp. 583–585. DOI: 10.1103/PhysRevLett.12.583 (cit. on p. 12).

[13] R. W. Damon and H. Van De Vaart. "Propagation of Magnetostatic Spin Waves at Microwave Frequencies in a Normally-Magnetized Disk." In: *Journal of Applied Physics* 36.11 (1965), p. 3453. DOI: 10.1063/1.1703018 (cit. on p. 12).

[14] A. Einstein. "Experimenteller Nachweis der Ampèreschen Molekularströme." In: *Naturwissenschaften* 3.19 (1915), pp. 237–238. DOI: 10.1007/BF01546392 (cit. on p. 3).

[15] A. Einstein and W. J. de Haas. "Experimental proof of the existence of Ampère's molecular currents." In: *Koninklijke Nederlandse Akademie van Wetenschappen Proceedings Series B Physical Sciences* 18 (Jan. 1915), pp. 696–711 (cit. on p. 3).

[16] James H. E. Griffiths. "Anomalous High-frequency Resistance of Ferromagnetic Metals." In: *Nature* 158.4019 (1946), pp. 670–671. DOI: 10.1038/158670a0 (cit. on p. 11).

[17] John D. Jackson. *Classical Electrodynamics Third Edition*. 3rd. Wiley, 1998 (cit. on p. 17).

[18] R. I. Joseph and E. Schlömann. "Theory of Magnetostatic Modes in Long, Axially Magnetized Cylinders." In: *Journal of Applied Physics* 32.6 (June 1961), pp. 1001–1005. DOI: 10.1063/1.1736149 (cit. on pp. 25, 28).

[19] R. I. Joseph and E. Schlömann. "Demagnetizing Field in Nonellipsoidal Bodies." In: *Journal of Applied Physics* 36.5 (1965), pp. 1579–1593. DOI: 10.1063/1.1703091 (cit. on p. 18).

[20] Richard I. Joseph. "Ballistic Demagnetizing Factor in Uniformly Magnetized Cylinders." In: *Journal of Applied Physics* 37.13 (1966), pp. 4639–4643. DOI: 10.1063/1.1708110 (cit. on p. 18).

[21] Richard I. Joseph and Ernst Schlömann. "Theory of Magnetostatic Modes in Long, Axially Magnetized Cylinders." In: *Journal of Applied Physics* 32 (1961). DOI: 10.1063/1.1736149 (cit. on pp. v, vii, 12, 35).

[22] M. L. Kales. "Modes in Wave Guides Containing Ferrites." In: *Journal of Applied Physics* 24.5 (1953), pp. 604–608. DOI: 10.1063/1.1721335 (cit. on p. 12).

[23] Frederic Keffer. "Spin Waves." In: *Ferromagnetism / Ferromagnetismus*. Ed. by Henricus Petrus Johannes Wijn. Vol. 4 / 18 / 2. Encyclopedia of Physics / Handbuch der Physik. Springer, Berlin, Heidelberg, 1966, pp. 1–273. DOI: 10.1007/978-3-642-46035-7_1 (cit. on pp. 8, 10).

[24] Charles Kittel. "Interpretation of Anomalous Larmor Frequencies in Ferromagnetic Resonance Experiment." In: *Physical Review* 71.4 (1947), pp. 270–271. DOI: 10.1103/PhysRev.71.270.2 (cit. on p. 11).

[25] Charles Kittel. "On the Theory of Ferromagnetic Resonance Absorption." In: *Physical Review* 73.2 (1948), pp. 155–161. DOI: 10.1103/PhysRev.73.155 (cit. on p. 11).

[26] L. Lehtonen, O. Vainio, J. Ahokas, J. Järvinen, S. Sheludyakov, K.-A. Suominen, and S. Vasiliev. "Searching for magnetostatic modes in spin-polarized atomic hydrogen." In: *Physica Scripta* 95.4 (Feb. 2020), p. 045405. DOI: 10.1088/1402-4896/ab6eb4 (cit. on p. 36).

[27] J. E. Mercereau and R. P. Feynman. "Physical conditions for ferromagnetic resonance." In: *Physical Review* 104.1 (1956), p. 63. DOI: 10.1103/PhysRev.104.63 (cit. on p. 11).

[28] J. A. Osborn. "Demagnetizing Factors of the General Ellipsoid." In: *Physical Review* 67 (June 1945), pp. 351–357. DOI: 10.1103/PhysRev.67.351 (cit. on p. 17).

[29] Sergio M. Rezende and Antonio Azevedo. "Dipolar narrowing of ferromagnetic resonance lines." In: *Physical Review B* 44.13 (1991), pp. 7062–7065. DOI: 10.1103/PhysRevB.44.7062 (cit. on p. 12).

[30] O. W. Richardson. "A Mechanical Effect Accompanying Magnetization." In: *Phys. Rev. (Series I)* 26 (3 Mar. 1908), pp. 248–253. DOI: 10.1103/PhysRevSeriesI.26.248 (cit. on p. 3).

[31] Baptiste Savoie. "A rigorous proof of the Bohr-van Leeuwen theorem in the semiclassical limit." In: *Reviews in Mathematical Physics* 27.08 (2015), p. 1550019. DOI: 10.1142/S0129055X15500191 (cit. on p. 3).

[32] Morgan Sparks. "Ferromagnetic resonance in thin films. I. theory of normal-mode frequencies." In: *Physical Review B* 1.9 (1970), pp. 3831–3856. DOI: 10.1103/PhysRevB.1.3831 (cit. on p. 12).

[33] Morgan Sparks. "Magnetostatic modes in an infinite circular disk." In: *Solid State Communications* 8.10 (1970), pp. 731–733. DOI: https://doi.org/10.1016/0038-1098(70)90419-9 (cit. on p. 12).

[34] Daniel D. Stancil and Anil Prabhakar. *Spin Waves: Theory and Applications*. Springer, 2009. DOI: 10.1007/978-0-387-77865-5 (cit. on pp. 3–5, 47, 48).

[35] K. J. Standley. "James Griffiths and Ferromagnetic Resonance." In: *Physics Bulletin* 34.3 (Mar. 1983), pp. 115–118. DOI: 10.1088/0031-9112/34/3/023 (cit. on p. 11).

[36] J. Van Vleck. "A Survey of the Theory of Ferromagnetism." In: *Reviews of Modern Physics* 17.1 (Jan. 1945), pp. 27–47. DOI: 10.1103/RevModPhys.17.27 (cit. on p. 5).

[37] Laurence R. Walker. "Magnetostatic Modes in Ferromagnetic Resonance." In: *Phys. Rev.* 105 (2 Jan. 1957), pp. 390–399. DOI: 10.1103/PhysRev.105.390 (cit. on pp. v, vii, 12).

[38] Pierre Weiss. "L'hypothèse du champ moléculaire et la propriété ferromagnétique." In: *J. Phys. Theor. Appl.* 6.1 (1907), pp. 661–690. DOI: 10.1051/jphystap:019070060066100 (cit. on p. 5).

[39] Robert L. White and Irvin H. Solt. "Multiple ferromagnetic resonance in ferrite spheres." In: *Physical Review* 104.1 (1956), pp. 56–62. DOI: 10.1103/PhysRev.104.56 (cit. on p. 11).